Immune check point blockade approach to metastatic prostate cancer treatment : improving existing and finding novel therapeutic modalities

Benzon, Benjamin

Doctoral thesis / Disertacija

2018

Degree Grantor / Ustanova koja je dodijelila akademski / stručni stupanj: **University of Split, School of Medicine / Sveučilište u Splitu, Medicinski fakultet**

Permanent link / Trajna poveznica: https://urn.nsk.hr/urn:nbn:hr:171:204974

Rights / Prava: In copyright/Zaštićeno autorskim pravom.

Download date / Datum preuzimanja: **2024-11-26**

University of Split

School of Medicine

Benjamin Benzon, M.D.

Immune check point blockade approach to metastatic prostate cancer treatment, improving existing and finding novel therapeutic modalities

PhD Thesis

Split, 2018.

University of Split

School of Medicine

Benjamin Benzon, M.D.

Immune check point blockade approach to metastatic prostate cancer treatment, improving existing and finding novel therapeutic modalities

PhD Thesis

Split, 2018.

Table of Contents

Abbreviation list

CTLA-4 – cytotoxic T lymphocyte antigen 4

PD-1 – programmed death 1

PD-L1 - programmed death ligand 1

ADT – androgen deprivation therapy

TNF-α – tumor necrosis factor alpha

IL-2 – interleukin 2

IFN-γ – interferon gamma

GS- Gleason score

MDSC- myeloid Derived Suppressor Cells

EGF- epidermal growth factor

FGF- fibroblast growth factor

IGF- insulin like growth factor

ERG- ETS-related gene

ETS- erythroblast transformation specific

SPNIK1- serine protease inhibitor Kazal-type 1

AUC- area under curve

ChIP- chromatin immunoprecipitation

GSEA – gene set enrichment analysis

DAVID- Database for Annotation, Visualization and Integrated Discovery

Introduction

Adenocarcinoma of prostate, problem overview

It is estimated that 2.5 million men will be diagnosed with prostate cancer between 2012. and 2017., which makes it most common cancer among men in industrialized world (1). Despite advances in treatment and early detection of local and regional disease it remains 3rd leading cause of cancer related death among men (1). In a setting of subclinical or clinical metastases androgen deprivation is considered frontline therapy. However, while many patients will experience initial tumor regression their prostate cancer inevitably develops castration resistant phenotype (2).

Processes which lead to prostate cancer resistance reflect astonishing ability of cancer to adapt to low androgen conditions. Upon deprivation of androgens many prostate cancer cells undergo apoptosis but some survive and experience arrest of cell cycle in G1 phase. The latter is thought to be mediated by stromal derived growth factors signaling such as FGF, KGF and IGF which causes androgen receptor (AR) stabilization and activation despite low levels of androgens in tissue (3). On the other hand, androgen deprivation abolishes the ARs auto negative feedback which leads to *AR* gene upregulation and de novo synthesis of androgens in cancer itself (4, 5). These adoptive changes cause disease progression in virtually all patients at a median time of 18 to 24 months. Next line of treatment is with so called 2nd generation anti androgens which either block local de novo synthesis of androgens or competitively bind to ligand binding site of AR and prevent its activation and translocation in to nucleus (3, 6). This more profound androgen supression causes cancer to regress again in some patients. However, in presence of profound androgen depletion cancer cells upregulate expression of alternative AR splice variants whose activity is independent of ligand binding (7). Furthermore, since normal AR and physiologic androgen levels induce differentiation of basal cells in prostate epithelia, long term androgen supression causes even more upregulation of genes associated with stem cell like properties (5). Consequently, after a year or 2 in the majority of responsive patients cancer becomes resistant to castration, again (2).

In a further effort to treat such patients multiple approaches have been undertaken. These include the development of third generation anti-androgens, chemotherapy and testing of pathway targeted small molecules as well as combing those with standard androgen ablation therapy in hormone naïve metastatic disease (8). Despite these novel strategies, the complexity of advanced tumors and their ability to adopt resistance often allows for further cancer progression and the patient's ultimate demise (9).

Conceptually speaking, the immune system which has function of dealing with adoptable and versatile entities such as pathogenic microorganisms, by definition emerges as a potential therapeutic tool in countering the problem of vast adaptability of prostate cancer and cancer in general.

Brief history of an immunological approach to cancer treatment

At the end of 19th century William B. Coley, an orthopedic surgeon from New York City, was first to systematically apply an immune based therapy to treat his cancer patients (10). Coleys treatment, a mixture of heat neutralized *S. pyogenes* and *S. marcescens,* yielded 5-year survival rates that were comparable to those of patients diagnosed with cancer in early 1980's (10, 11). However, since at that time immunology was at very nascent stage and tumor immunology was nonexistent, Coley could not postulate a mechanism of action for his treatment which along with the emergence of radiation and chemotherapy caused his treatment to gradually fall in to obscurity by the mid-20th century (12).

In 1943. Gross did a first tumor transplantation experiment in inbred mice in which he showed that mice can be successfully immunized to syngeneic chemically induced tumor and that immunity against tumor is specific for the type of tumor (13). In next 3 decades investigations on similar models demonstrated some basic concepts in cancer immunology: tumors are heterogeneous in their antigenicity (14); spontaneous tumors are less immunogenic then chemically and virally induced tumors (15); cellular immunity is crucial for anti-tumor response (16); tumors can suppress immune responses directed against them and induce tolerance (17); suboptimal immune response against tumor can facilitate tumor growth (18). Parallelly with these investigations, in 1959. Ruth and John Graham launched first cancer vaccine trial ever, 114 patients with gynecologic cancers were treated with autologous tumor lysate augmented by Freunds adjuvant. The treatment induced remission or disease stabilization in 22% of patients, despite these results trial went largely unnoticed (19).

During the 1970's basic immunology saw major progress in identifying fundamental mechanisms of immune system function. Doherty and Zinkernagel postulated MHC restriction mechanism (20), dendritic cells were discovered and their antigen presenting function was characterized (21), NK cells were also characterized (22, 23), IL-2 was purified and characterized as a growth factor for lymphocytes (24). One of the most far-reaching achievements of this period was proposal of 2 signal lymphocyte activation model by Lafferty and Cunningham (25). These discoveries along with industrial production of IL-2, IFN-α and IFN-γ, which was made possible due to

recombinant DNA technology, formed a basis for some of the landmark clinical trials in next decade (26).

In 1985., after promising results in murine model of metastatic cancer and phase I trials, Rosenberg et al. applied recombinant IL-2 with adoptive transfer of peripheral blood lymphocytes in phase II trial which yielded 23% and 33% response rates in patients with metastatic melanoma and renal cell carcinoma (27). Later trials showed that same results can be obtained by high dose IL-2 therapy alone (28). By the end of a decade same group also launched a new kind of treatment with adoptive transfer of ex-vivo expanded tumor infiltrating lymphocytes, which in combination with IL-2 doubled the response rates in comparison to IL-2 monotherapy (29). IFN-α was another cytokine that showed some efficacy in treatment of hematologic malignances (30). In 1989. after a 60 years of basic and clinical investigations BCG treatment for bladder cancer was approved, thus becoming first FDA approved immunotherapy for cancer (31). In the realm of basic immunology "2 signals " hypothesis was experimentally validated by functional characterization of MHC and T cell receptor interactions as "signal 1" along with CD28 and CD80/CD86 interactions as "signal 2" (32).

Led by structural homology in their search for new CD80 and CD86 ligands Lindley et al. came across CTLA-4, at the time a newly identified molecule (33). Same group demonstrated that CTLA-4 has 20-fold higher avidity for CD80 and CD86 molecules then CD28 (34). Finally, four years later in 1995. Allison and Krummel elucidated the function of CTLA-4 as a competitive antagonist of CD28 (35). A year later Allison and Leach showed, in murine models of various cancers, that blocking CTLA-4 could be a feasible immunologic strategy against tumors (36); this would mark cancer immunotherapy research for next 20 years. Last decade of 20th century also saw further development of IL-2 and adoptive cell transfer treatments in metastatic melanoma and renal cell carcinoma. However, despite a great theoretical potential and established proofs of principles in cytokine, vaccine and adoptive cell transfer trials few patients experienced long term benefit (37). To explain such results Ephraim Fuchs and Poly Matzinger proposed a model in which the absence of costimulatory signal or "signal 2" induces anergy and tolerance in anti-tumor lymphocytes (38). Furthermore, they pointed out to the absence of so called "danger signals", i.e. signals that are induced by the cell injury and death or the by imminent danger to cell, as a cause of downregulation of costimulatory molecules on antigen presenting cells. This model also raised a possibility that local ablative therapies such as radiation or thermal ablation might trigger systemic immune response and thus eradicate tumor at sites distant from original ablation area. Such phenomena, called "the abscopal effect", were reported throughout 20th century but their immune dependent mechanism remained unproven until 2004. (39). The very end of 20th century was marked by elucidation of cancer immunosuppressive mechanisms. Honjo et. al characterized PD-1/ PD-L1 interaction and its

role in tumor induced immunosuppression (40). Immature myeloid cells that were associated with cancer related immunosuppression were fully characterized and named myeloid derived suppressor cells, furthermore T regulatory lymphocytes were also fully characterized and their role in cancer immunosuppression was elucidated (41, 42).

21st century saw translation of anti-CTLA-4 and anti-PD-1 antibodies, now dubbed immune check point inhibitors, in to clinical trials and eventually in to clinical practice (43). In 2005. a phase I/II trial of CTLA-4 blocking antibody named ipilimumab yielded 22% objective response rate in metastatic melanoma (44). This trial was followed by a phase III trial, also in metastatic melanoma patients, yielding 20% overall survival rates after 4 years of follow up which resulted in FDA approval in 2011 (45). First phase I/II trial of anti-PD-1 was published in 2012. yielding 28% objective response for metastatic melanoma, 18% for non-small cell lung cancer, 27% for renal cell carcinoma (46). Phase II or III trials fallowed soon, resulting in anti-PD-1 treatment approval for metastatic melanoma, NSCLC, RCC, head and neck cancer and Hodgkin lymphoma by 2017. (47-51). In addition to blocking inhibitory check points and thus "lifting the brakes", many clinical trials today are combining agonists of costimulatory immune check points such as vaccines or agonistic antibodies and therefore "pushing the gas paddle" of immune system (52, 53). Furthermore, based on case report by Postow et al. (54) and animal studies (55) several clinical trials seeking to elicit the abscopal effect by combining local ablative therapies and immune checkpoint inhibition have launched in a recent time (ClinicalTrials.gov #: NCT03323424, NCT02115139, NCT02535988, NCT02542930).

Prostate cancer immunology and immune therapy

Unlike melanoma and kidney cancer, immunotherapies for prostate cancer have showed only marginal efficacy. The only currently approved immunotherapy for prostate cancer is dendritic cell vaccine called Sipilucel T. Sipilucel T prolongs median survival for 4 to 5 months in patients with mCRPC, but eventually all patients progress and die (56). CTLA-4 blockade in metastatic prostate cancer showed promising results in one of phase II trials, on the other hand a follow up phase III trial showed only marginal benefit with median survival prolongation of 1 month (57). In one of first anti PD-1 phase II trials patients with prostate cancer did not show any signs of objective response (46). These findings point out to low immunogenicity of prostate cancer.

Low immunogenicity of prostate cancer was also described in recent genome wide analysis of immune microenvironment in various cancers (58). In this study a proxy measure of cytolytic activity of immune cells was among lowest in prostate cancer (Figure 1a). Reasons for such low immunogenicity may be in low mutational burden of prostate cancer (Figure 1b) (59). Furthermore,

some patients with metastatic prostate cancer have high levels of MDSCs and T regulatory cells in blood which in turn affects their prognosis unfavorably (60). On the other hand, more detailed investigations of prostate cancer microenvironment in terms of immune related pathways, especially the checkpoint molecules and their interactions with other oncogenic pathways are lacking.

Tumors can be made more immunogenic by serval strategies, one of which is ablating the tumor. Tumor ablation increases concentrations of "danger signal" molecules and consequently causes upregulation of the costimulatory molecules on lymphocytes and antigen presenting cells (39, 55, 61). Previous work has demonstrated that among ablative therapies, cryotherapy causes a particularly robust immune response. For example, Waltz et al. demonstrated in an immune re-challenge experiment with an androgen independent mouse model of prostate cancer that cryoablation of tumors synergizes with high dose (10 mg/kg) anti CTLA-4 antibody treatment (62). Cryotherapy has also been reported to elicit distant anti-tumor effects in case reports of human malignancies including prostate cancer (63, 64). In addition to tumor ablation and vaccination, drug induced mutagenesis, depletion of MDSCs, epigenetic manipulations and androgen deprivation might also augment immunity to tumor (65-67).

Therefore, this thesis has two objectives first one is to characterize prostate cancer immune microenvironment using the high throughput methods, second one is to find optimal combination of local ablative or systemic therapy with the immune checkpoint blockade in terms of safety and efficacy.

a)

b)
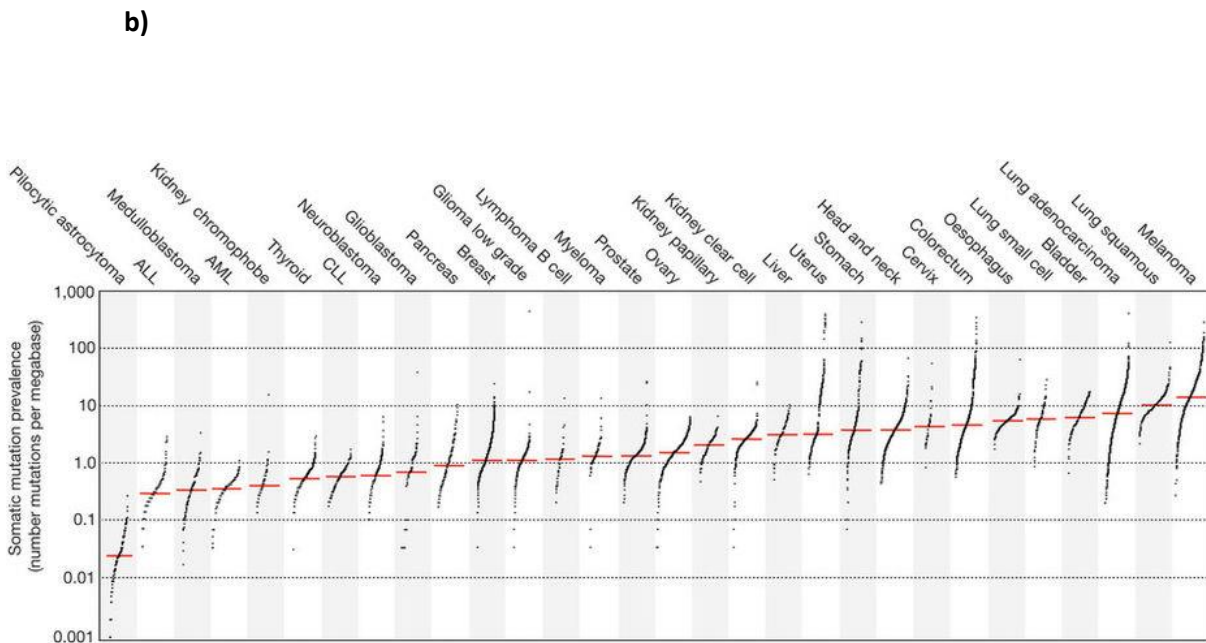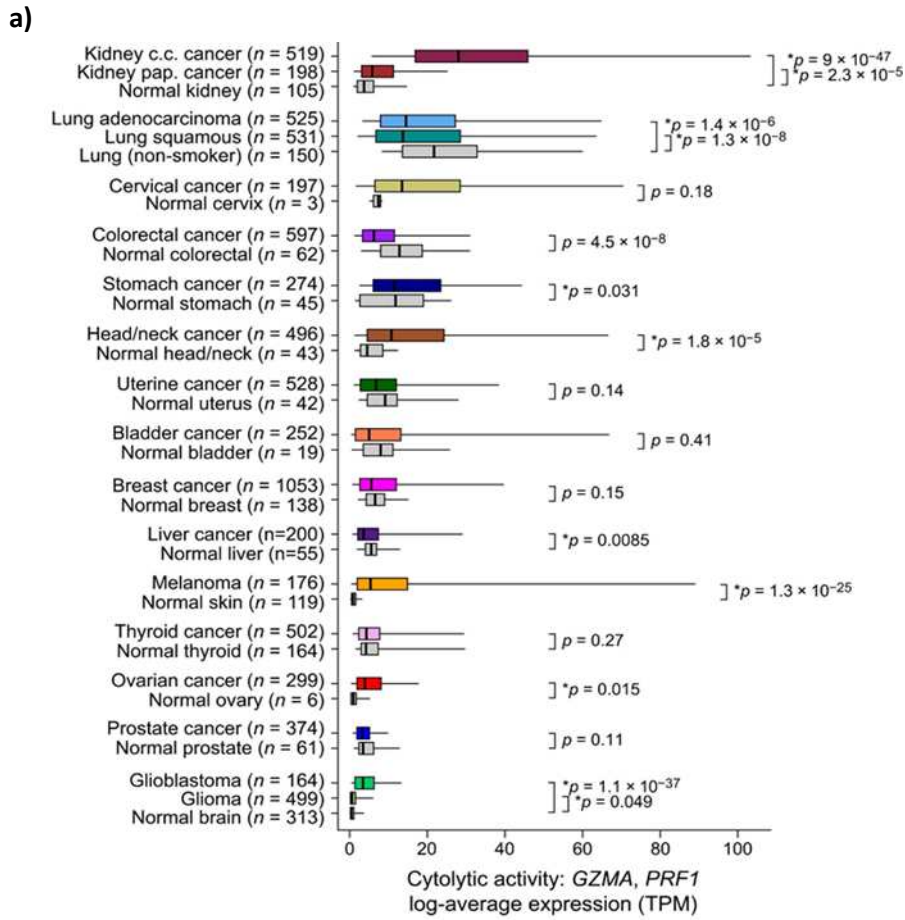
Figure 1. a) Cytolytic activity of immune cells in various cancers,
after (58). **b)** Mutational burden of some cancers, after (59)

Aims

Characterization of prostate cancer immune microenvironment.

Characterize prostate cancer immune environment by searching for immune genes that are related to oncologic outcomes and construct their interactome with more detail considerations on their relations to immune pathways and to the other cellular pathways which represent targets for the mainstay therapeutic modalities in prostate cancer (e.g. androgen deprivation therapy).

Improving efficacy of immune check point inhibitors

Test in immunocompetent murine model of androgen sensitive metastatic prostate cancer which, if any, of local ablative therapies (cryoablation, radiation, surgery) synergizes with one of the following: PD-1 blockade, high (10mg/kg) dose CTLA4 blockade and low (1mg/kg) dose CTLA4 blockade. Since PD-1 blockade is thought to be less potent then CTLA-4 blockade boosting PD-1 blockade with a single dose of androgen deprivation or epigenetic modulation therapy is also investigated.

Patients, Materials and Methods

Patients, Materials and Methods in "Prostate Cancer Immune Microenvironment Characterization" Study

Patient Cohorts

Prostatectomy tissue was derived from two patient cohorts (Figure 2). The first included prostatectomy samples with associated genomic information from 2,111 patients prospectively submitted for clinical Decipher testing (68). A second cohort included prostatectomy tissue from 670 patients that had undergone radical prostatectomies at the Johns Hopkins Hospital (JHH). In the patients from JHH, two case-cohort designs were used to investigate clinical outcomes: (1) a case-cohort based on 260 men with intermediate or high risk localized prostate cancer undergoing prostatectomy at JHH and then followed expectantly until clinical metastasis (69), and (2) a case cohort natural history study of 211 patients who had biochemical recurrence after prostatectomy but did not receive therapy until the time of metastasis.

Prostatectomy Sample Selection and Processing

Specimen selection, RNA extraction, and microarray hybridization was done in a Clinical Laboratory Improvement Amendments (CLIA)-certified laboratory facility (GenomeDx Biosciences, San Diego, CA, USA) as previously described (69, 70). Briefly, total RNA was extracted and purified using the RNeasy FFPE kit (Qiagen, Valencia, CA). RNA was amplified and labeled using the Ovation WTA FFPE system (NuGen, San Carlos, CA) and hybridized to Human Exon 1.0 ST GeneChips (Affymetrix, Santa Clara, CA).

Quality control was performed using Affymetrix Power Tools, and normalization was performed using the Single Channel Array Normalization (SCAN) algorithm (71). Gene expression was summarized using the Affymetrix core transcript cluster and corrected for batch effects using an empirical Bayes framework (ComBat in R package sva_3.14.0).

Chromatin immunoprecipitation

Publicly available datasets of AR chromatin immunoprecipitation (ChIP)-Seq experiments were analyzed using IGV (72, 73). Chromatin immunoprecipitation experiments were performed as described previously (74). In brief, formaldehyde cross-linked LNCaP cells were subjected to immunoprecipitation with AR specific antibodies (Millipore, Darmstadt,

Germany) or control IgG (Cell Signaling Technologies, Danvers, MA, USA) after 8 h of 100 nM dihydrotestosterone (DHT, Sigma Aldrich, St. Louis, MO, USA) or solvent control treatment. Enriched libraries were amplified using primers specific to the putative upstream regulatory site (upstream, F: 5′-GCTTTTATGAGCCTCCGTGA-3′; R:5′AGCACTGAGCCATTCACCTT-3′) and the transcriptional start site (TSS, F: 5′CGTCCCTGAGTCCCAGAGT-3′; R: 5′-GGTTCCCGGGACTCCTGT-3′). Data are shown as relative enrichment normalized to input DNA. Primers specific to the KLK3 locus (which encodes for PSA and harbors a well characterized AR-binding site) were used as a control.

Androgen-dependent expression of B7-H3 in prostate cancer cell lines

LNCaP cells were grown in RPMI and either charcoal stripped fetal bovine serum (FBS) (deprived of androgens), FBS (contains androgens) or charcoal stripped FBS supplemented with DHT. Cells were harvested and B7-H3 expression was assayed using quantitative reverse transcription PCR with Taqman assays. All experiments were done in quadruplicate. LNCaP cells were obtained from ATCC, authenticity was validated by STR profiling and cells were confirmed as mycoplasma free by the MycoAlert Mycoplasma Detection Kit (Lonza, Basel, Switzerland).

Statistical Analysis

Predictive power of genes for oncological outcomes (biochemical recurrence, metastases, overall and prostate cancer specific mortality) was evaluated by logistic regression and ROC analysis. Genes with AUC (c index) greater than 70% for any of oncologic outcomes were considered for detailed analysis.

B7H3 expression distribution was compared to the expression of 3 other known checkpoint molecules. Survival analysis (R package survival_2.38-3) was performed in the JHH cohorts to evaluate the prognostic value of B7H3 and to compare the prognostic value of the 4 ligands. Numbers at risk were adjusted according to the case-cohort design of the studies (75). To test the association of B7H3 expression with clinicopathologic variables, Kruskall-Wallis tests (R package stats_3.2.1) and boxplots were used. Associations of B7H3 expression with molecular subtypes (ERG+, ERG-ETS+, ERG-SPINK1+, TripleNeg) (76) were evaluated using Pearson's correlation. The association of B7H3 expression with AR was assessed using Pearson's correlation and ChIP seq analysis. Statistical analyses were

17

performed in R, version 3.2.1 and all statistical tests were two-sided using a 5% significance level and interpreted according to 2016. ASA Statement on p-values.

Functional characterization and GSEA

Associations of B7-H3 expression with 104 genes which are a part of Nanostring's nCounter PanCancer Immune Profiling Panel were evaluated using Pearson's correlation and p-values were adjusted using Holm's method. Genes were ranked based on their Pearson's correlation to B7H3 in the prospective cohort and GSEA was carried out to identify gene sets associated with B7H3 by using the GSEA analysis tool (version 2.2.0) downloaded from the Broad Institute website (http://www.broadinstitute.org/gsea/index.jsp). The curated gene sets of the Molecular Signature Database (MSigDB) version 4.0 was used for enrichment. The FDR for GSEA is the estimated probability that a gene set with a given NES (normalized enrichment score) represents a false-positive finding, and an FDR <0.25 is considered to be statistically significant for GSEA. The Database for Annotation, Visualization and Integrated discovery (DAVID) was used to evaluate molecular concepts enriched in genes which were highly correlated with *B7-H3* (77).
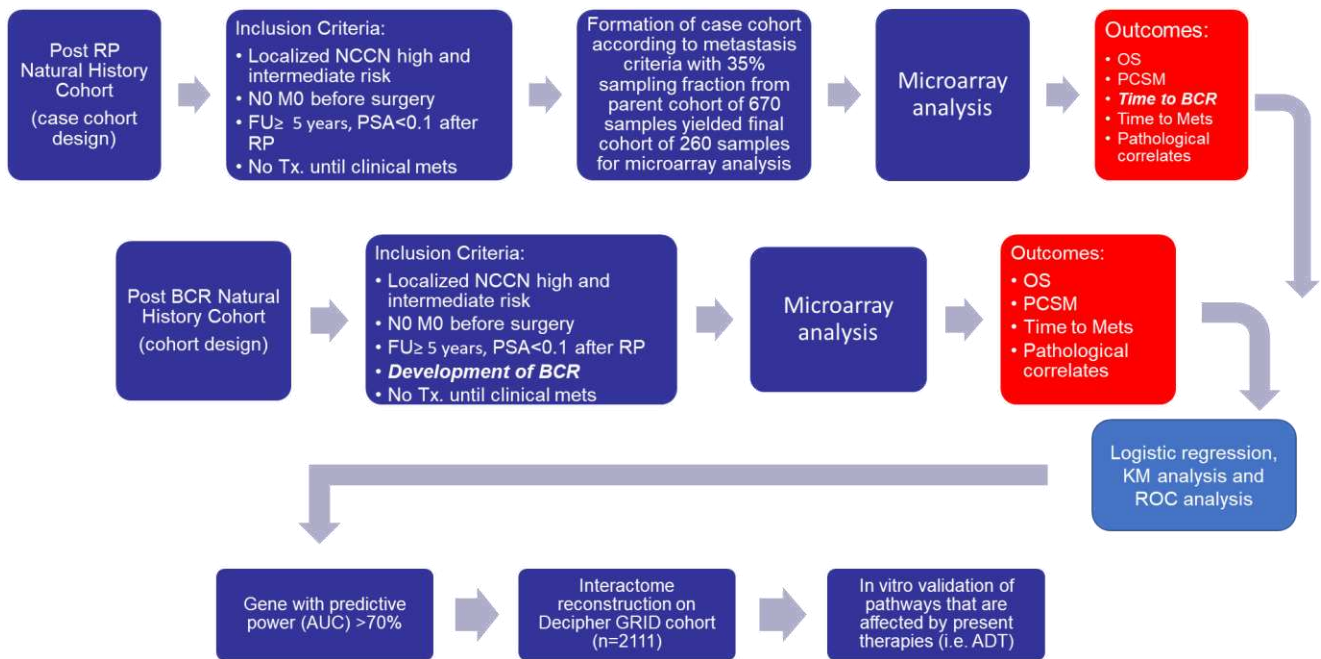
Figure 2. A design of Prostate Cancer Immune Microenvironment Characterization Study.

Legend: NCCN- National Comprehensive Cancer Network; FU- fallow up

Materials and Methods in the Study of "Improving Immune Check Point Blockade in the Treatment of Metastatic Prostate Cancer"

Mice and tumor cells

All experimental procedures were approved by the Johns Hopkins Institutional Animal Care and Use Committee (IACUC).   Immune –competent 7 to 11 weeks old male FVB/NJ mice (Jackson Laboratories, Bar Harbor, ME, USA) were used in all experiments. Two synchronous grafts were formed by subcutaneous (s.c.) injection of $1\cdot10^6$ and $0.2\cdot10^6$ Myc-Cap cells into the right and left flank, respectively (cells were obtained by courtesy of Dr. Simons).

Tumor Growth and Survival Measurements

Tumor grafts were measured with calipers every two to three days starting on the 14th day after cells injection, graft volume was calculated by formula $V = \frac{x\cdot y^2}{2}$, with x denoting the longer diameter and y denoting shorter diameter of tumor graft. Mice were sacrificed when they became moribund or if tumor size reached 2000 mm³.

Tumor ablation

In experimental groups where ablation was employed, it was performed on the larger graft only and was performed with the intent to treat the complete tumor area of that graft. Grafts were ablated two days after checkpoint inhibitor (or isotype control) treatment initiation. In the case of mice receiving androgen deprivation therapy, tumors were ablated 6 days after ADT initiation. Cryoablation was carried out using Cryocare machine (HeathTronics, Austin, TX, USA). Mice were anesthetized by 2.5% isoflurane gas anesthesia. Once anesthetized, skin overlaying the larger tumor graft was disinfected with

alcohol pads and a single 8 mm cryoablation probe was inserted. In all cases, 2 freeze-thaw cycles were delivered with temperatures at the probe tip reaching a minimum of negative 40°C for at least 30 s. Mice were provided all necessary post procedural care.

For irradiation and surgical resection mice were anesthetized and prepared as it is described previously. Larger isograft was irradiated with either a single dose of 10 Gy or 3 fractions of 3.3 Gy delivered in 3 consecutive days by external beam from SARRP machine (Xstrahl Ltd., Camberley, Surrey, UK). Surgical excision was done as en block excision of larger isograft.

Immune check point blocking, Androgen deprivation therapy and Epigenetic modifiers

InVivoMAb Anti-mouse PD-1 (10mg/kg, clone J43, Bioxcell, West Lebanon, NH, USA), InVivoMAb anti-mouse CTLA-4 antibody (1mg/kg, clone 9H10, Bioxcell), or InVivoMAb hamster anti-mouse IgG control antibodies (clone N/A, catalog # BE 0091, Bioxcell) were administered every other day for a total of four doses by intra-peritoneal (i.p.) injection. The first dose was administered upon the larger tumors reaching 100 to 200 mm^3, except for mice allocated to groups receiving androgen deprivation therapy in which case first dose was given 4 days after initiation of androgen deprivation therapy. When employed, androgen deprivation was induced by degarelix (Ferring Pharmaceuticals, Saint Prex, Switzerland), administered in single s.c. dose of 25 mg/kg upon the larger tumor graft reaching a volume of 300-400 mm^3.

Entinostat and 5 azacytidine, when employed, were administered at the same schedule as immune check point blockade via i.p. route at the dose of 0.8 mg/kg and 22 mg/kg, respectively.

Immuno-depletion

Depletion of all CD3$^+$ lymphocytes, or CD8$^+$ lymphocytes was performed as described in Belcaid et al (78). Briefly, we utilized i.p. injection of InVivoMAb anti-mouse CD3 (clone 2.43, Bioxcell) and InVivoMAb anti-mouse CD8 (clone 145-2C11, Bioxcell) antibodies at doses of 100 μg and 200 μg, respectively. Induction of depletion was performed by using six doses of antibodies given every second day. Following the sixth dose, depletion was maintained by administering one dose of depleting antibody per week. The first dose of depleting antibody was given 5 days before larger tumors reached 100 to 200 mm^3 or 300 to 400 mm^3 in case of group treated with androgen deprivation therapy. Confirmation of depletion was obtained by flow cytometric analysis of blood after the second dose of antibodies was administered.

Flow cytometry

Two weeks after cryotherapy or the second dose of check point blocking antibody, tumors, spleens, and tumor draining lymph nodes were dissected from the mice. In order to obtain tumor infiltrating lymphocytes tumors were mechanically disassociated and digested for 1h at 37°C in RPMI media with 10 mg/ml of Collagenase IV and 1mg/ml of DNase. After digestion, white blood cells were isolated from tumors by using anti CD45 antibodies conjugated with magnetic beads (Miltenyi Biotec, Bergisch Gladbach, Germany) according to manufacturer's instructions. Lymph nodes and spleens were disrupted mechanically, washed and suspended as single cell solution in media. Tumors, spleens and lymph nodes from 2 mice, from the same group, were pooled in one sample and all experiments were conducted utilizing at least 6 mice.

In order to stain for intracellular cytokines, lymphocytes were stimulated for 5 h with PMA (100 ng/ml), ionomycin (500 ng/ml), and Protein transport inhibitor cocktail

(eBioscience, San Diego, CA, USA) at 37°C. Cells were permeabilized and fixed with

Intracellular Fixation & Permeabilization Buffer Set (eBioscience, San Diego, CA, USA). Data

were acquired on FACS Aria II machine (BD Biosciences, San José, CA, USA). Staining was

performed by using antibodies against CD4 (clone H129.19, BD Biosciences), CD8 (clone 53-

6.7, BD Biosciences), IFNγ (clone XMG 1.2, eBioscience), TNFα (clone MP6-XT22,

eBioscience), IL-2 (clone JES6-5H4, eBioscience), FoxP3 (clone FJK-16s, eBioscience). Staining

for immune checkpoint molecules was done on a separate panel with antibodies to CD4

(clone H129.19, BD Biosciences), CD8 (clone 53-6.7, BD Biosciences), PD-1 (clone J43,

eBioscience), Tim-3 (clone RMT3-23, eBioscience) and Lag-3 (clone C9B7W, eBioscience).

Gating controls were prepared with Fluorescence Minus One (FMO) stains of spleenocytes.

All data were analyzed with FlowJo software (TreestarInc, Ashland, OR, USA).

Statistical analysis

Statistical differences in Kaplan Meier survival curves were evaluated with log rank

testing and hazard ratio estimation. Tumor growth curves were analyzed by fitting

segmental linear (broken stick) model with two segments (79-81). Briefly, time to

accelerated or fast growth is a model parameter defined as the "changepoint" or

"breakpoint" and is the time at which tumor started to grow at a faster average rate (Figure

3b). Pairwise Mann Whitney test was used to test differences in medians and F- test was

used to compare standard deviations, for comparisons of means pairwise t test was used.

Significance of linear trend between groups was evaluated with linear trend test. P values

less than 0.05 were considered significant, all P values were two-sided, P values were

interpreted according to 2016. ASA statement on P values. Sample size was estimated by

using Mead's resource equation. Allocation was done by using complete randomization. All

statistical analysis was done in Grapad Prism 6.07 software (GraphPad Software, La Jolla, CA, USA).

*Establishing a Mouse Model to Evaluate the Abscopal Effect*

The Myc-CaP cell line was derived from primary prostate cancer developed in a Myc over-expressing transgenic mouse model and is isogenic on the FVB mouse background (82). To establish a simple model with which to test for the abscopal effect, we subcutaneously injected both flanks of immune competent mice (Figure 3). One flank was implanted with 1 million cells while other was implanted with 200,000 cells. Upon the larger tumor reaching a volume of 100 to 400 mm^3 (approximately 3 to 4 weeks after injection), mice were allocated into 3 different treatment arms (Figure 3A). Mice allocated to first arm received either anti PD-1 antibody or isotype control, with or without ablation of larger tumor (Figure 3A). The second experimental group was designed identically as the first but employing an anti- CTLA-4 antibody instead of anti PD-1 antibody. In the third arm experimental group, a single dose of androgen deprivation therapy with degarelix was added to the treatment regimen of the first arm. When the effect of epigenetic modification was tested entinostat and 5 AZA were added to arms with PD-1 blockade. In experimental groups where ablation was employed, this model would allow for straightforward assessment of growth of the distant untreated graft.

24
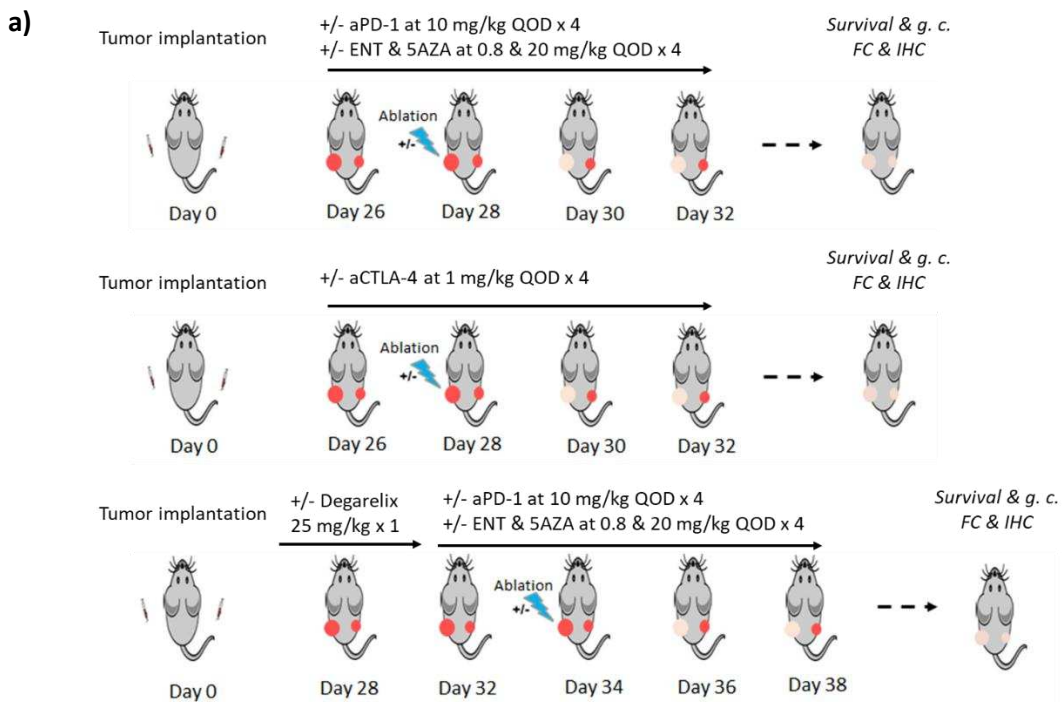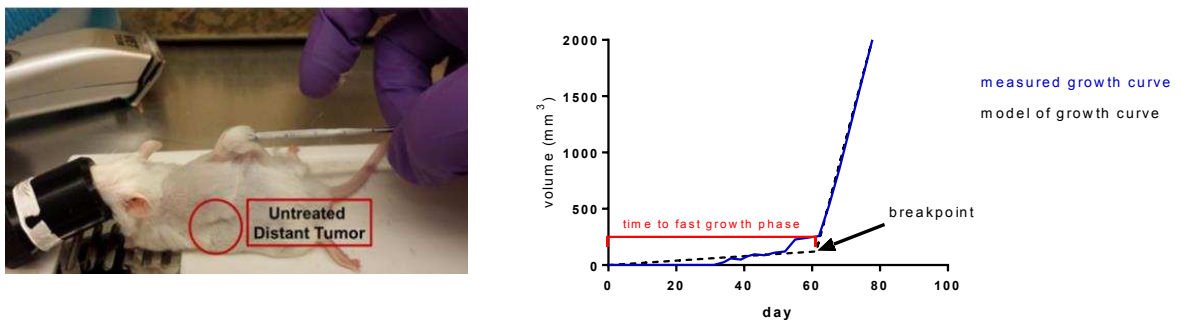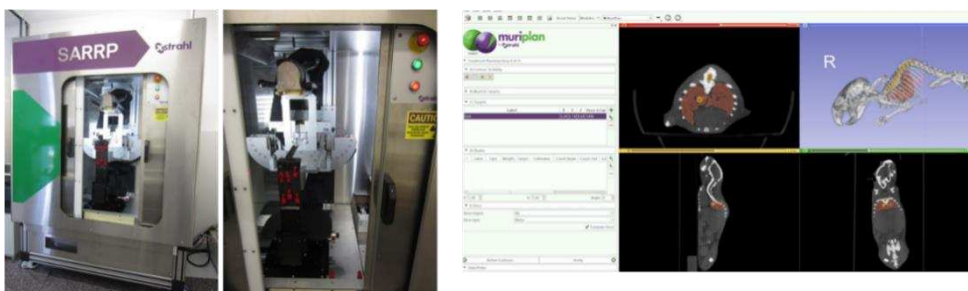
Figure 3. a) Design of Improving of Immune Check Point Blockade in Metastatic Prostate Cancer Treatment Study. Ablation of tumor with cryosurgery and growth curve modelling **(b)**; external beam radiation **(c)**.

Legend: *g.c., growth curves; FC, flow cytometry; IHC, immune-histochemistry; ENT, etinostat; 5AZA, 5' azacytidine*

Results

Results from "Characterization of Prostate Cancer Immune Microenvironment" Study

35 immune genes (Table 1) were tested according to their predictive values for oncologic outcomes, only *B7-H3* showed AUC above 70% and statistically significant prognostic characteristics, thus it was the only gene considered in further analysis.

Relationship of B7-H3 and Immune Ligands to Prostate Cancer as well as Pathologic and Clinical Outcomes

When compared to benign prostatic tissue, *B7-H3* expression is significantly higher in prostate cancers (p<0.04) (Figure 4a). In order to further examine B7-H3 expression in prostate cancer, we analyzed 2111 prostatectomy samples for which micro-array data was available. Median *B7-H3* expression was within the top 81 percentiles of genes expressed in prostate cancer and was 2.5-fold higher than the median expression for all genes. In contrast, and concordant with previous studies, *PD-L1*, *PD-L2* and *B7-H4* were not highly expressed in prostate cancer (Figure 4b). Expression of *B7-H3* varied according to stage and grade, with median expression increasing among those men with primary Gleason pattern 4 or Gleason sum 8-10 disease (Fig 4c, d). We additionally found increasing expression with increased pathological stage (p<0.02). *B7-H3* expression was also significantly increased in castrate resistant metastatic prostate cancer when compared to localized disease (Figure 4e).

To determine the correlation between increased *B7-H3* expression and oncologic outcomes following surgery we performed Kaplan-Meier analysis for metastatic events based on median split of *B7-H3* expression in cohorts for which long term follow up was available. Among men who underwent prostatectomy and then had no further treatment until the time of metastasis, higher *B7-H3* expression (but not *PD-L1*, *PD-L2* or *B7-H4* expression) was significantly associated with metastatic outcome (Figure 5a). We additionally analyzed a separate case-cohort study of men who underwent radical prostatectomy and developed biochemical recurrence but had no further treatment until metastatic progression. Among these men, who are higher risk of overall metastatic progression, increased *B7-H3* expression also significantly correlated with the development of clinical metastasis (Figure 5b). Higher *B7-H4* expression in this cohort appeared

protective but this did not meet statistical significance (p=0.06) (data not shown). On multi-variable analysis in either cohort, level of *B7-H3* expression was not a significant independent predictor of prostate cancer outcomes, likely due to the positive correlation of *B7-H3* expression levels with grade and stage (Table 2a, b).

Table 1. List of genes used to characterize prostate cancer immune microenvironment

GENE	DESCRIPTION	PROGNOSTIC VALUE	C INDEX (AUC) > 70%
IDO1	immune modulator/possibly master regulator	none	no
PDCD1	checkpoint	none	no
CD274	checkpoint (expressed on tumors)	none	no
PDCD1LG2	checkpoint (expressed on tumors)	none	no
CTLA4	checkpoint	none	no
HAVCR2	checkpoint	bcr, pcsm	no
LAG3	checkpoint	none	no
FOXP3	Treg marker	none	no
CXCL9	T cell chemokine	bcr, met, pcsm	no
CCL5	T cell chemokine	none	no
CD80	co-stimulatory molecule	bcr, met, pcsm	no
CXCL13	B cell chemokine	met, pcsm	no
IGKC	Ig Kappa light chain on B cells	bcr, met, pcsm	no
CR2	Complement receptor B cells	bcr, met, pcsm	no
TNF	T cell activation marker (regulatory/cyotoxic)	bcr, met, pcsm	no
GZMB	T cell activation marker (cytotoxic)	bcr	no
IL2	T cell activation marker	none	no
TNFRSF4	costimulatory	bcr, met, pcsm	no
CD40	costimulatory	none	no
CD27	TNF receptor	none	no
TNFRSF9	T cell activation marker (regulatory/cytotoxic)	mets, pcsm	no
BTLA	checkpoint	bcr, pcsm	no
ADORA2A	checkpoint	bcr, met, pcsm	no
VTCN1	checkpoint	none	no
CD276 (B7H3)	**checkpoint**	**bcr, met, pcsm**	**yes**
CD3	T cell marker	none	no
CD4	T cell marker	none	no
CD8A; CD8B	T cell marker	met, pcsm	no
MS4A1	B cell marker	bcr, met, pcsm	no
CD79A	B cell marker (recognizes plasma cells)	bcr, met, pcsm	no
NCAM1	NK cell marker	bcr, met, pcsm	no
ITGAM	myeloid marker	none	no
CD33	myeloid marker	met, pcsm	no
FCGR1A	macrophage marker	bcr, met, pcsm	no

Legend: Prognostic value, significance of Kaplan Meier analysis result for one of oncological outcomes; bcr, biochemical recurrence; met, radiologic metastases; pcsm, prostate cancer specific mortality
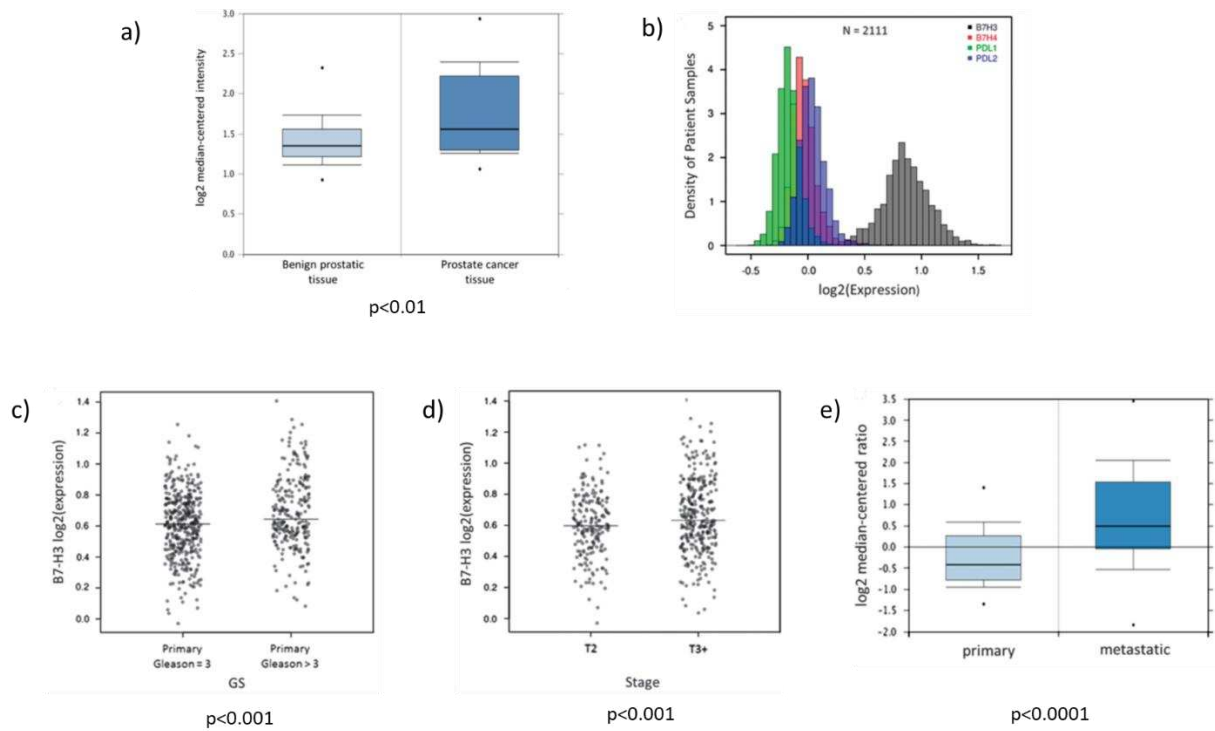
Figure 4. (a) B7-H3 expression in benign and cancerous prostate tissue. **(b)** Expression distributions of B7-H3, B7-H4, PD-L1 and PD-L2 in a prospective radical prostatectomy (RP) cohort (n =2111). **(c, d)** Dot plots showing B7-H3 expression is higher in more aggressive tumors as it is significantly associated with pathologic Gleason grade and tumor stage. **(e)** Box plots showing B7-H3 expression is associated with metastasis as expression is higher in metastatic tumors vs to primary tumors. Data for this comparison were derived from Oncomine consisting of 59 primary tumor samples and 34 metastatic castration resistant prostate cancer tumor samples

Legend: GS, Gleason score.
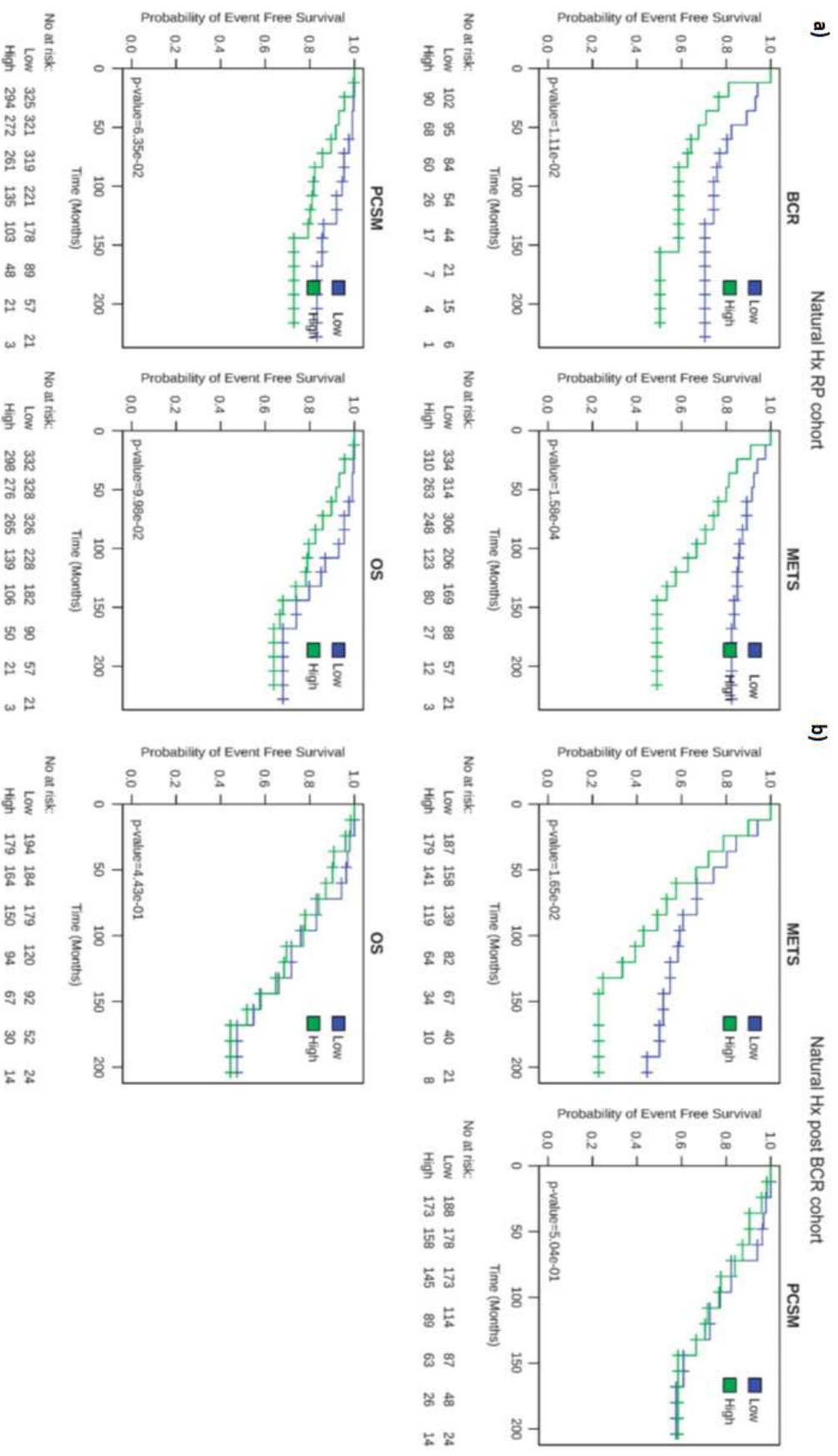
Figure 5. (a) Kaplan–Meier curves for biochemical recurrence (BCR), clinical metastasis (METS), prostate cancer specific mortality (PCSM) and overall survival (OS) in a natural history prostate cancer radical prostatectomy (RP) cohort. **(b)** Kaplan–Meier curves in a natural history RP cohort of patients that developed BCR after RP.

30

Table 2. a) Analysis of *B7-H3* as prognostic marker for metastasis with continuous variables in logistic model.

Cohort	Variable	Univariable analysis		Multivariable analysis	
		OR (95%CI)	p value	OR (95%CI)	p value
Natural Hx RP	**B7H3**	1.71 (1.33 - 2.20)	**<0.001**	1.19 (0.83 - 1.70)	0.34
	GS	2.71 (2.09 - 3.51)	**<0.001**	2.23 (1.64 - 3.04)	**<0.001**
	LNI	2.09 (1.67 - 2.63)	**0.00**	1.40 (1.01 - 1.94)	**0.04**
	SM	1.26 (1.01 - 1.57)	**0.04**	0.88 (0.64 - 1.21)	0.43
	ECE	1.87 (1.39 - 2.53)	**<0.001**	1.44 (1.00 - 2.06)	0.05
	SVI	2.26 (1.80 - 2.85)	**<0.001**	1.49 (1.10 - 2.01)	**0.01**
	PSA	1.17 (0.96 - 1.43)	0.12	1.02 (0.81 - 1.27)	0.89
	AGE	0.93 (0.74 - 1.16)	0.52	1.03 (0.74 - 1.42)	0.88
Natural Hx post BCR	**B7H3**	1.47 (1.17 - 1.83)	**<0.001**	1.06 (0.80 - 1.40)	0.68
	GS	2.26 (1.79 - 2.85)	**<0.001**	2.14 (1.64 - 2.80)	**<0.001**
	LNI	1.41 (1.15 - 1.74)	**<0.001**	1.03 (0.78 - 1.35)	0.84
	SM	0.92 (0.74 - 1.14)	**0.44**	0.78 (0.61 - 1.00)	0.05
	ECE	1.37 (1.09 - 1.72)	**0.01**	1.00 (0.74 - 1.35)	1.00
	SVI	1.73 (1.39 - 2.14)	**<0.001**	1.61 (1.23 - 2.10)	**<0.001**
	PSA	1.14 (0.92 - 1.41)	**0.23**	0.99 (0.77 - 1.28)	0.95
	AGE	0.96 0.78 - 1.19	**0.74**	0.94 (0.73 - 1.21)	0.62

Legend: OR, odds ratio; GS, Gleason Score; LNI, Lymph node involvement; SM, surgical margin; ECE, extracapsular extension; SVI, seminal vesicles involvement; PSA, prostate specific antigen.

Table 2. b) Analysis of *B7-H3* as prognostic marker for metastasis with categorical variables in logistic model

Cohort	Variable	Univariable analysis		Multivariable analysis	
		OR (95% CI)	p value	OR (95% CI)	p value
Natural Hx RP	**B7H3.Q2**	0.91 (0.44 - 1.91)	0.80	1.41 (0.54 - 3.73)	0.49
	B7H3.Q3	1.93 (0.98 - 3.79)	0.06	2.13 (0.88 - 5.12)	0.09
	B7H3.Q4	3.08 (1.58 - 6.00)	**<0.001**	2.19 (0.84 - 5.75)	0.11
	GS8+	6.12 (3.65 - 10.26)	**<0.001**	4.19 (2.18 - 8.05)	**<0.001**
	LNI	6.23 (3.54 - 10.97)	**<0.001**	3.07 (1.41 - 6.67)	**<0.001**
	SM	1.67 (1.02 - 2.73)	**0.04**	0.97 (0.49 - 1.95)	0.94
	ECE	3.97 (2.06 - 7.64)	**<0.001**	2.18 (0.98 - 4.86)	0.06
	SVI	6.14 (3.67 - 10.27)	**<0.001**	2.30 (1.16 - 4.57)	**0.02**
	PSA10to20	0.97 (0.58 - 1.61)	0.90	2.05 (1.01 - 4.19)	0.05
	PSA20+	1.45 (0.71 - 2.96)	0.31	1.55 (0.56 - 4.28)	0.40
	AGE	0.99 (0.95 - 1.02)	**0.52**	1.01 (0.96 - 1.07)	0.59
Natural Hx post BCR	**B7H3.Q2**	1.28 (0.68 - 2.40)	0.44	0.85 (0.42 - 1.72)	0.64
	B7H3.Q3	1.44 (0.77 - 2.68)	0.25	0.90 (0.45 - 1.80)	0.76
	B7H3.Q4	2.67 (1.45 - 4.92)	**<0.01**	1.19 (0.58 - 2.46)	0.63
	GS8+	4.82 (3.05 - 7.61)	**<0.001**	4.01 (2.38 - 6.74)	**<0.001**
	LNI	2.18 (1.36 - 3.5)	**<0.001**	1.01 (0.54 - 1.89)	0.96
	SM	0.84 (0.54 - 1.31)	0.44	0.65 (0.39 - 1.09)	0.10
	ECE	2.02 (1.2 - 3.4)	**0.01**	1.04 (0.54 - 2.00)	0.90
	SVI	3.20 (2.03 - 5.05)	**<0.001**	2.76 (1.55 - 4.91)	**<0.001**
	PSA10to20	1.08 (0.66 - 1.75)	0.77	1.23 (0.70 - 2.15)	0.47
	PSA20+	1.34 (0.67 - 2.67)	0.41	1.11 (0.48 - 2.56)	0.81
	AGE	0.99 (0.96 - 1.03)	**0.74**	0.99 (0.95 - 1.04)	0.68

Legend: OR, odds ratio; GS, Gleason Score; LNI, Lymph node involvement; SM, surgical margin; ECE, extracapsular extension; SVI, seminal vesicles involvement; PSA, prostate specific antigen.

Relationship of B7-H3 to Androgen Receptor Signaling

We investigated the relationship between *B7-H3* expression and molecular subtypes of prostate cancer. *B7-H3* expression appeared to increase among patients with ERG+ disease and decrease among triple negative patients (Figure 6a). A positive correlation between ERG+ status and *B7-H3* expression suggested a relationship between *B7-H3* and androgen receptor signaling. We explored this in our prospective cohort and found a positive correlation between *AR* expression and *B7-H3* expression (Figure 6b), with *B7-H3* being among the most correlated genes with AR expression (85th percentile) and visa versa (79th percentile) (Figure 6c and d). A similar finding was demonstrated in the JHMI cohorts with Pearson correlation coefficients of 0.47. In gene set enrichment analysis, the androgen receptor signaling pathway was positively correlated with B7-H3 expression (normalized enrichment score=1.62 and 1.90 p=0.05 and <0.001 for the prospective and JHMI cohorts respectively) (Figure 7). We next evaluated whether AR occupancy could be seen in the 5' UTR of B7-H3 by examining ChIP sequencing data. In the presence of androgen (R1881), ChIP sequencing data suggested AR binding upstream of B7-H3 in androgen dependent prostate cancer cell lines (LNCaP and VCaP) (Figure 8). To address the functional consequence of AR binding upstream of *B7-H3* we evaluated the expression of *B7-H3* under different conditions in the LNCaP prostate cancer cell line. LNCaP cells grown in RPMI supplemented with FBS (which contains androgens) show low expression of *B7-H3* compared with cells grown in medium supplemented with charcoal stripped FBS (deprived of androgens). Conversely, expression of *B7-H3* was greatly reduced in LNCaP cells grown in charcoal stripped FBS, which was supplemented with DHT. These findings, shown in Figure 8c, suggest that androgen receptor binding negatively regulates *B7-H3* expression.

Given the relationship between B7-H3 and AR, we conducted an exploratory analysis using genes having a Pearson's correlation coefficient >0.5 between B7-H3 and AR and used DAVID to functionally cluster those genes. Enriched clusters included genes involved in cell cycle, cell differentiation, proteolysis, apoptosis, splicing and DNA repair, as well as those associated with the androgen receptor and WNT (Figure 9).

33
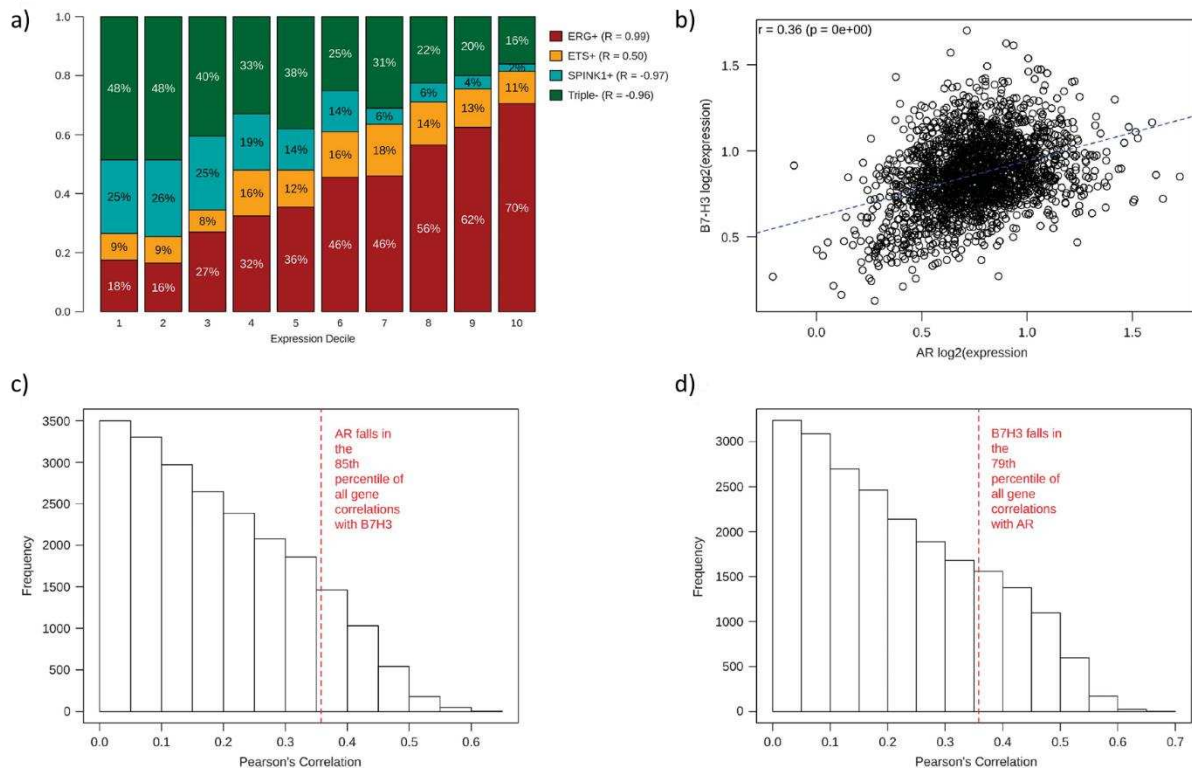
Figure 6. a) B7-H3 expression trends with the molecular subtype in samples from a prospective RP cohort (n=2111). **b)** B7-H3 expression positively correlates with AR expression when measured in a prospective cohort (n= 2111, R =0.36). **c)** AR is among the most correlated genes with B7-H3 (85th percentile). **d)** B7-H3 is among the most correlated genes with androgen receptor (AR; 79th percentile). RP, radical prostatectomy.
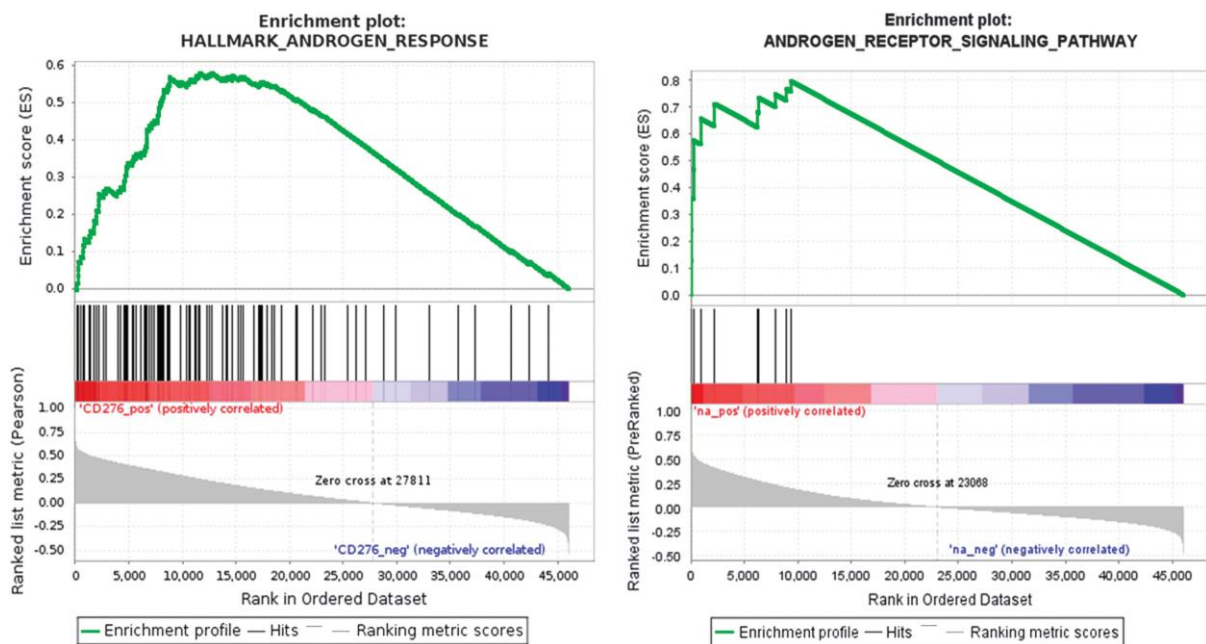

Figure 7. Gene set enrichment analysis in the prospective cohort (left) and Johns Hopkins Medical Institute (JHMI) natural history cohorts (right) shows the androgen receptor signaling pathway is positively correlated with B7-H3 expression.
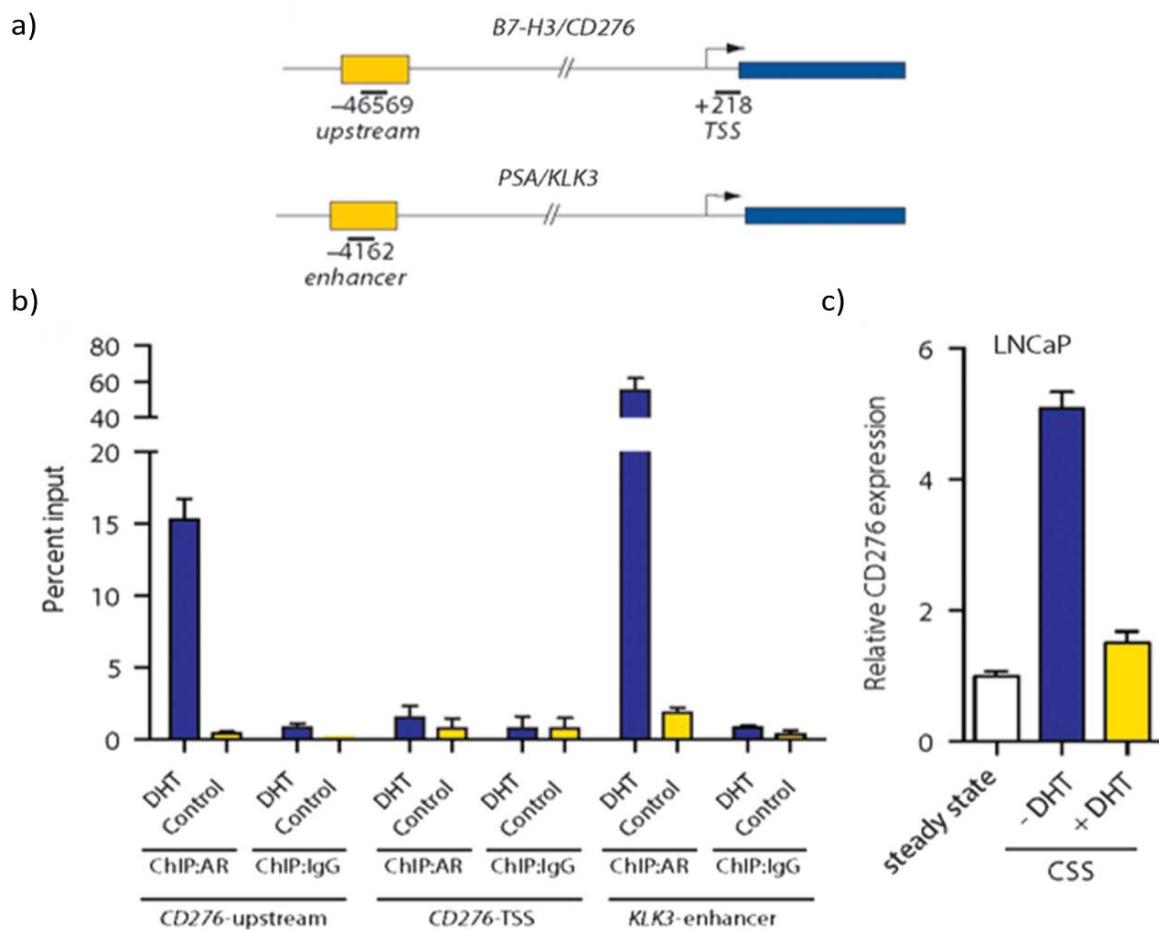
Figure 8. Androgen-induced binding of the androgen receptor (AR) to a putative regulatory element upstream of B7-H3/CD276. **(a)** Schematic of primer locations (bars indicate primer positions relative to transcriptional start sites (TSS)). **(b)** AR binding sites were identified by mining previously published ChIP-Seq data. Chromatin precipitation was performed using LNCaP cells grown in the absence of androgens and treated for 8 h with 100 nM DHT or solvent control. Cell lysates were incubated with anti-AR or IgG control antibodies and precipitated DNA was analyzed using primers specific to an upstream region of B7-H3/CD276 or the B7-H3/CD276 promoter (TSS). Enrichment at the KLK3/PSA enhancer is shown as a positive control. Data are shown normalized to total DNA input for each amplicon. **(c)** Expression of B7-H3 as assayed by quantitative reverse transcription (qRT-PCR) in LNCaP cells grown in RPMI supplemented with FBS (which contains androgens), RPMI supplemented with charcoal stripped FBS (deprived of androgens), or RPMI with charcoal stripped FBS, which was supplemented with DHT.

Legend: FBS, fetal bovine serum; CSS, charcoal striped serum.
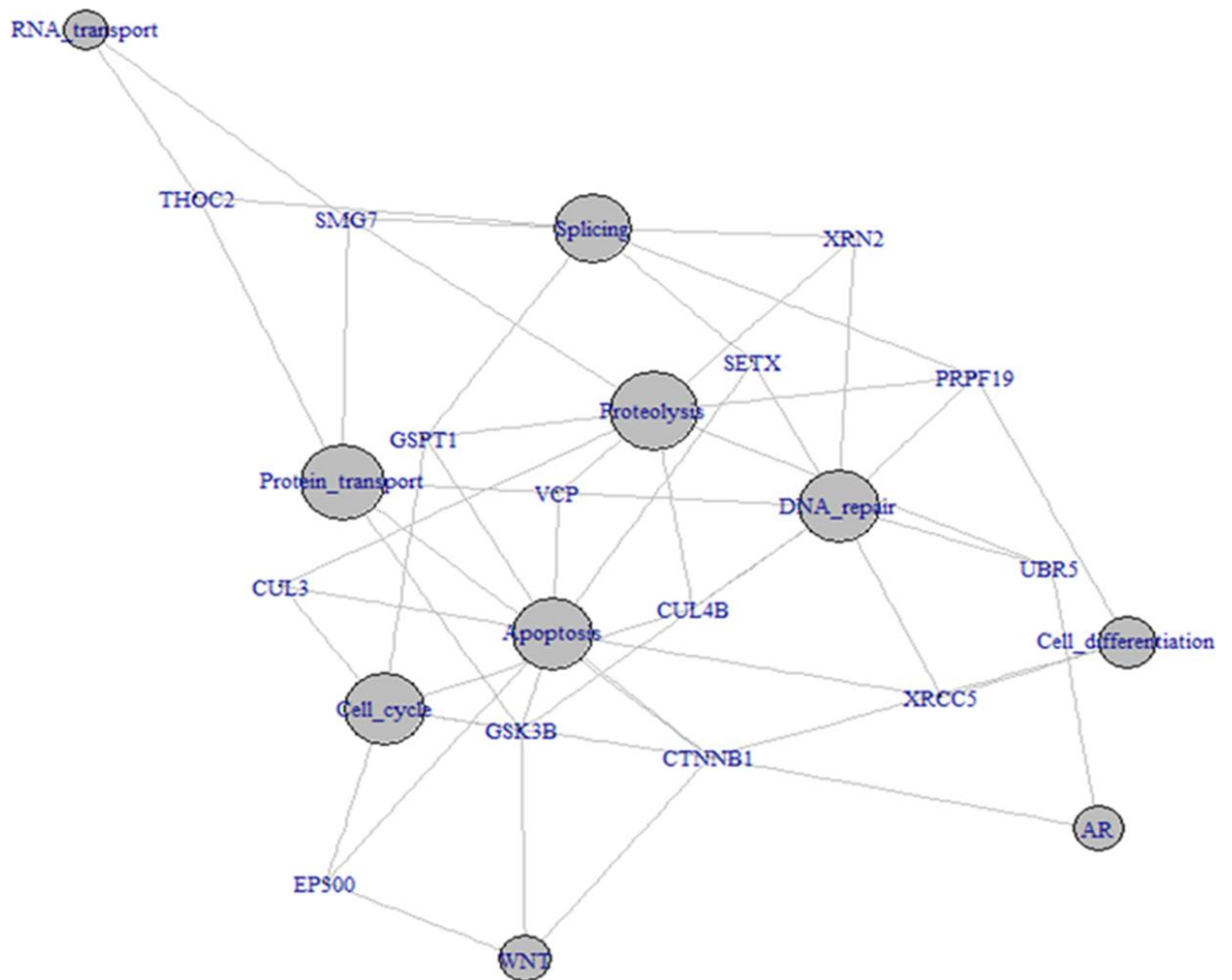
Figure 9. *In silico* interaction network between *B7-H3* and *AR* constructed from genes that showed Pearson correlation coefficient >0.5 with B7-H3 and AR, genes were functionally clustered according to DAVID.

Legend: AR, androgen receptor; DAVID, Database for Annotation, Visualization and Integrated Discovery

Gene Set Enrichment Analysis and Immune Gene Correlations with B7-H3 Expression

In order to define putative relationships and functions for *B7-H3*, we performed unbiased gene set enrichment analysis using the prospective cohort. Positively enriched gene sets are shown in Table 3. No significantly negatively correlated gene set was found. Because of B7-H3's role in immune modulation we were particularly interested in the enrichment of immune pathways. Significantly enriched immune related gene sets included TGF-Beta signaling and IL2-STAT5 signaling pathways (NES 1.64 and 1.6 respectively, adj p<0.05 for both). To further explore the associations between *B7-H3* and immune related genes we investigated the correlation between *B7-H3* gene expression and expression of genes within a previously described immune panel (http://www.nanostring.com/products/pancancer_immune/). Supporting the enrichment of the TGF-beta signaling pathway, we saw positive correlations between B7-H3 expression and SMAD2, IL17RA, RORC and FoxP3 (Figure 10).

Table 3 Enriched gene sets among genes that correlate with B7-H3.

Gene set	Size	Enrichment Score	Normalized Enrichment Score	FDR q-value
PI3K AKT MTOR SIGNALING	105	0.64	1.91	0.02
MTORC1 SIGNALING	199	0.63	1.83	0.01
MYC TARGETS V1	199	0.72	1.80	0.02
P53 PATHWAY	199	0.56	1.79	0.02
WNT BETA CATENIN SIGNALING	42	0.62	1.76	0.02
NOTCH SIGNALING	32	0.65	1.72	0.02
TGF BETA SIGNALING	54	0.61	1.64	0.03
IL2 STAT5 SIGNALING	199	0.49	1.60	0.04
HEDGEHOG SIGNALING	36	0.52	1.59	0.05
ANDROGEN RESPONSE	100	0.58	1.58	0.05

Legend: FDR, false discovery rate
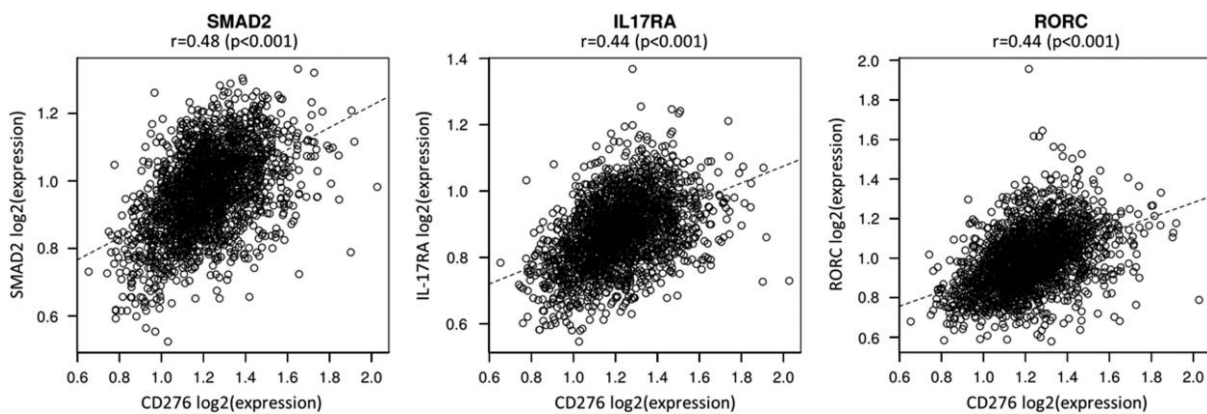
Figure 10. Pearson's correlation analysis shows positive correlations between *B7-H3* expression and *SMAD2, IL17RA* and *RORC* in the prospective cohort.

# Results from the Study of "Improving Immune Check Point Blockade in Treatment of Metastatic Prostate Cancer"

Cryoablation delays distant tumor growth but does not synergize with PD-1 blockade

Cryoablation of the larger tumor graft delayed onset of accelerated growth of the untreated tumor graft (median increase 9.83 days, 95% CI 3.2-18.81, p=0.0205) and caused almost 8-fold decrease in mortality rates (HR=0.126, 95% CI 0.0372-0.427, p=0.0009) when compared to an untreated control group (Figure 11a and Figure 12a). Anti PD-1 monotherapy did not show any effect in terms of delaying tumor growth nor did it improve survival when compared to control group. Combining PD-1 blockade with cryoablation did not show a synergistic effect when compared to cryoablation therapy alone (Figure 11a).

Cryoablation synergizes with low dose anti CTLA-4 treatment in a T cells dependent fashion

We next tested whether anti-CTLA-4 therapy might synergize with cryoablation to cause an abscopal effect. In a pilot experiment, we found that anti-CTLA-4 administered in concentrations of 10mg/kg caused a delay in tumor growth and improvement in mouse survival (Figure 13). Treatment with anti CTLA-4 at doses of 1mg/kg however, did not improve survival nor did it delay growth of tumor grafts (Figure 11b and Figure 12b). Cryoablation appeared to synergize with low dose (1 mg/kg) anti CTLA-4, delaying the onset of accelerated growth in remaining graft for 14.7 days (95% CI 9.98-21.58, p=0.0006) and decreasing mortality rate by factor of 4 (HR=0.25, 95% CI 0.0782-0.784, p=0.0003) when compared to cryoablation alone (Figure 11b and Figure 12b). Depletion of CD3$^+$ or CD8$^+$ cells in mice prior to treatment completely neutralized the beneficial effects of cryoablation and anti CTLA-4 combinatorial therapy, with mortality rates being comparable to control mice (Figure 11b). Depletion experiments also demonstrated that mice depleted of CD3+ or CD8+ cells and treated with combination of cryoablation and anti CTLA-4 had significantly lower survival rates when compared to mice treated with cryoablation alone (p=0.0251, p=0.0480, respectively).
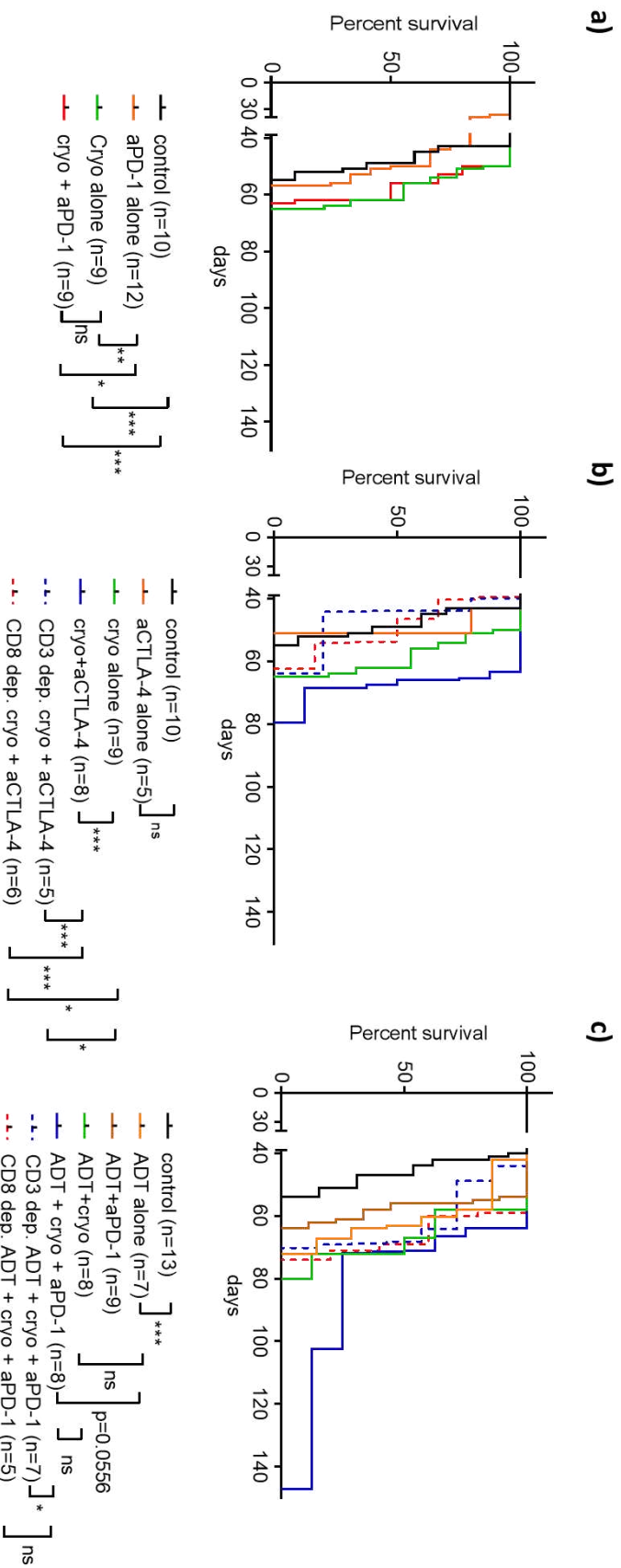
Figure 11. Kaplan Meier curves for mice from all therapeutic groups. a) Anti-PD-1 treatment did not synergize with cryoablation. **b)** Low dose anti-CTLA-4 synergized with cryoablation in a CD3 and CD8 dependent fashion. **c)** Combination of ADT and anti-PD-1 synergized with cryoablation in a CD3 and CD8 dependent fashion. Differences between mortality curves were tested by log rank test. Each treatment regimen was done with at least one experimental replicate.

*ns- p>0.05, * p<0.05, ** p<0.01, *** p<0.001*

a)

Ctrl vs aPD1 alone

Ctrl vs cryo alone

Ctrl vs cryo + aPD1

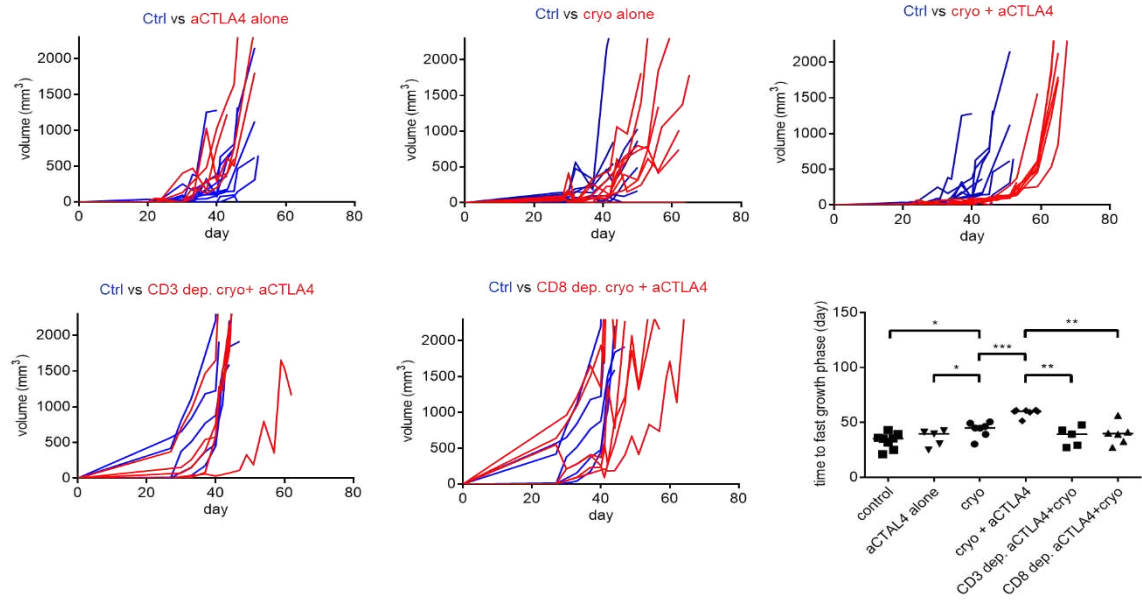b)

Ctrl vs aCTLA4 alone

Ctrl vs cryo alone

Ctrl vs cryo + aCTLA4

Ctrl vs CD3 dep. cryo+ aCTLA4

Ctrl vs CD8 dep. cryo + aCTLA4

c)

Ctrl vs ADT alone

Ctrl vs ADT +aPD1

Ctrl vs ADT+ cryo

Ctrl vs ADT + cryo+aPD1

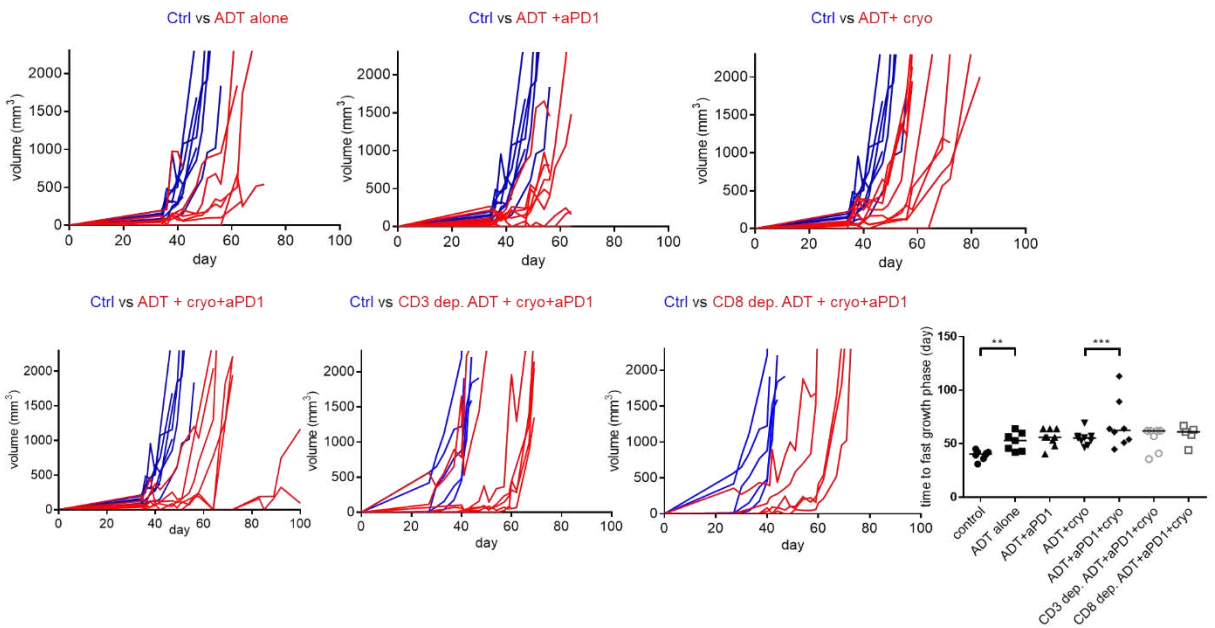Ctrl vs CD3 dep. ADT + cryo+aPD1

Ctrl vs CD8 dep. ADT + cryo+aPD1

41
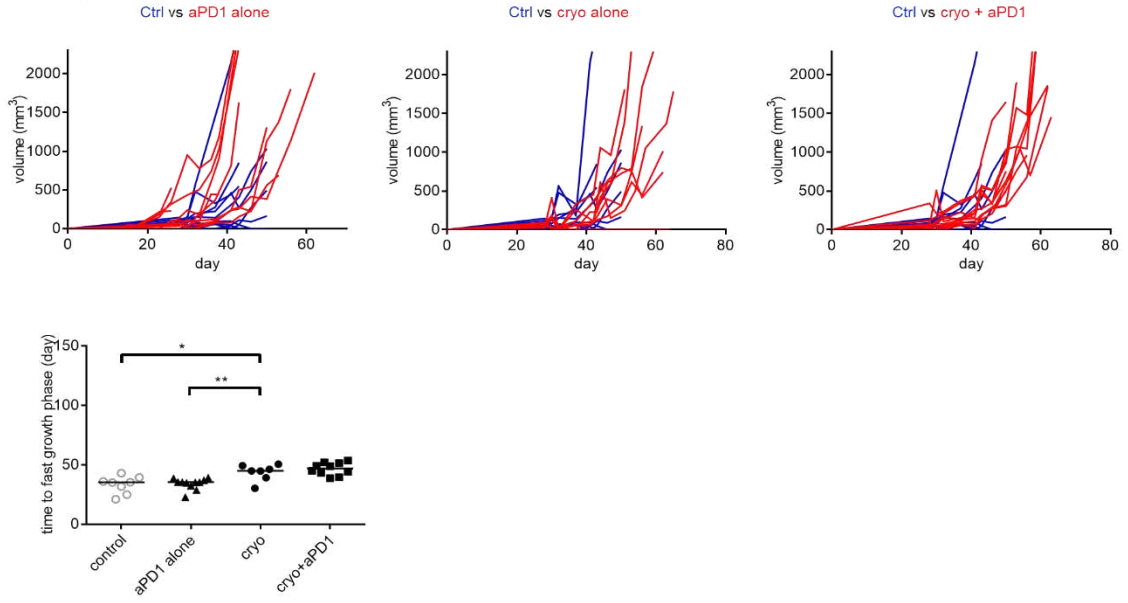
←**Figure 12. Growth curves of smaller tumor grafts. a)** Anti-PD1 and cryoablation combination did not delay onset of tumor accelerated growth more than cryoablation monotherapy. **b)** Low dose anti-CTLA-4 and cryoablation synergized and significantly delayed onset of accelerated tumor growth, in both CD3 and CD8 dependent manner, compared to cryoablation and anti-CTLA-4 monotherapies. **c)** Combination of ADT and anti-PD-1 synergized with cryoablation and delayed onset of tumor fast growth phase in 25% (2/8) of mice in a CD3 and CD8 dependent fashion when compared to the ADT and cryoablation combination. Statistical comparisons in terms of medians were done by using MW test, F test was used to compare standard deviations of groups. Each treatment regimen was done with at least one experimental replicate.

ns- p>0.05, * p<0.05, ** p<0.01, *** p<0.001
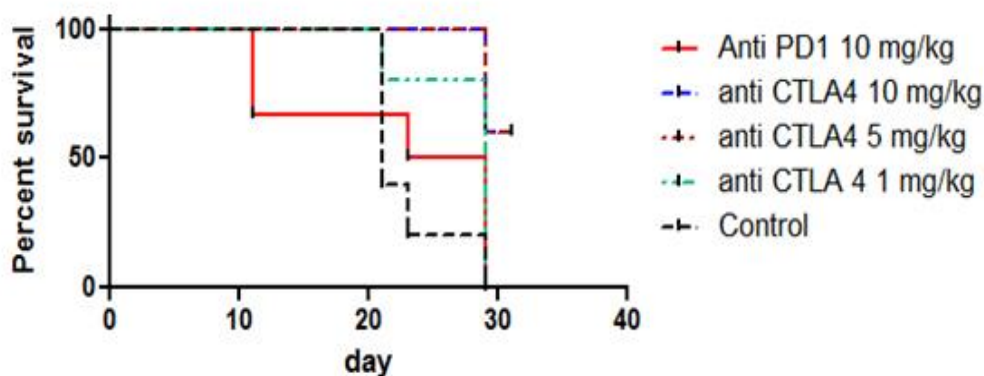
Figure 13. Results of dose titration pilot experiment. On this graph days are counted from the beginning of treatment unlike other KM graphs in this study in which days are counted from the moment of tumor cells implantation.

Androgen ablation therapy and anti PD-1 treatment synergize with cryoablation in a T cells dependent fashion in a subset of mice

Androgen deprivation therapy (ADT) has been previously shown to correlate with an increased prostate cancer tumor lymphocytic infiltrate and to mitigate tolerance to prostate cancer antigens(67, 83, 84). We tested whether addition of neoadjuvant ADT could synergize with anti-PD-1 based treatment to improve oncologic efficacy (Figure 11c and Figure 12c). As expected ADT alone postponed the onset of fast growth phase for 12.6 days (95% CI 2.57-21.91, p=0.0022) and caused 7.5-fold reduction in mortality rate (HR=0.131, 95% CI 0.041-0.42, p=0.0006). Combining ADT with anti PD-1 therapy did not show additional beneficial effects when compared to ADT monotherapy. Adding ADT to cryoablation resulted in non-significant survival benefit (HR=0.56, 95% CI 0.19-1.64, p=0.1720) and also non-significant tumor growth delay of 2.82 days (95% CI -7 to 12.43, p=0.5360) in comparison treatment with ADT alone (Figure 11c). Trimodal therapy consisting of ADT, PD-1 blockade and cryoablation almost doubled the delay of tumor growth (p=0.0021) and survival in 25% (2/8) of treated mice when compared to bi-modal therapy with ADT and cryoablation combination, however survival differences in these two experimental groups were not statistically different when all mice in each experimental group were considered (HR=0.798, 95% CI 0.297-2.142, p=0.6049) (Figure 11c). In order to study the nature of survival prolongation in mice treated by trimodal therapy we depleted mice of CD3$^+$ or CD8$^+$ cells and treated them with ADT, anti PD-1, and cryoablation combination therapy. In these immune-depleted mice, no mice experienced long term treatment response. Mice depleted of CD3$^+$ cells demonstrated significantly lower survival when compared to non-depleted mice treated with identical therapy (HR=4.015, 95% CI 1.098 - 14.68, p=0.0356), however survival difference between mice depleted of CD8$^+$ cells and non-depleted mice failed to reach statistical significance (HR=2.202, 95% CI 0.5937-8.165, p=0.2378).

To further investigate the nature of partial response in trimodal therapy group we hypothesized, based on Schaue et al. (85), that amount of tissue damage caused by cryoablation might offset the immune response towards anti-inflammatory phenotype, so we analyzed relationship between the volume of ablated tumor graft and length of life (Figure 14a). Trimodal therapy group showed that long term response to treatment, in

terms of lifespan decays exponentially, to levels identical to those of ADT and cryoablation group, with the rising volume of ablated tumor graft (R^2=98.7%, p=0.0131). Bi-modal therapy with cryoablation and ADT also showed exponential trend, although much weaker, of a slightly increased efficacy with decreasing ablated graft volume (R^2=40%, p=0.07). Other therapeutic regimes that contained cryoablation did not show any association between response to treatment and volume of cryoablated graft (Figure 14b).
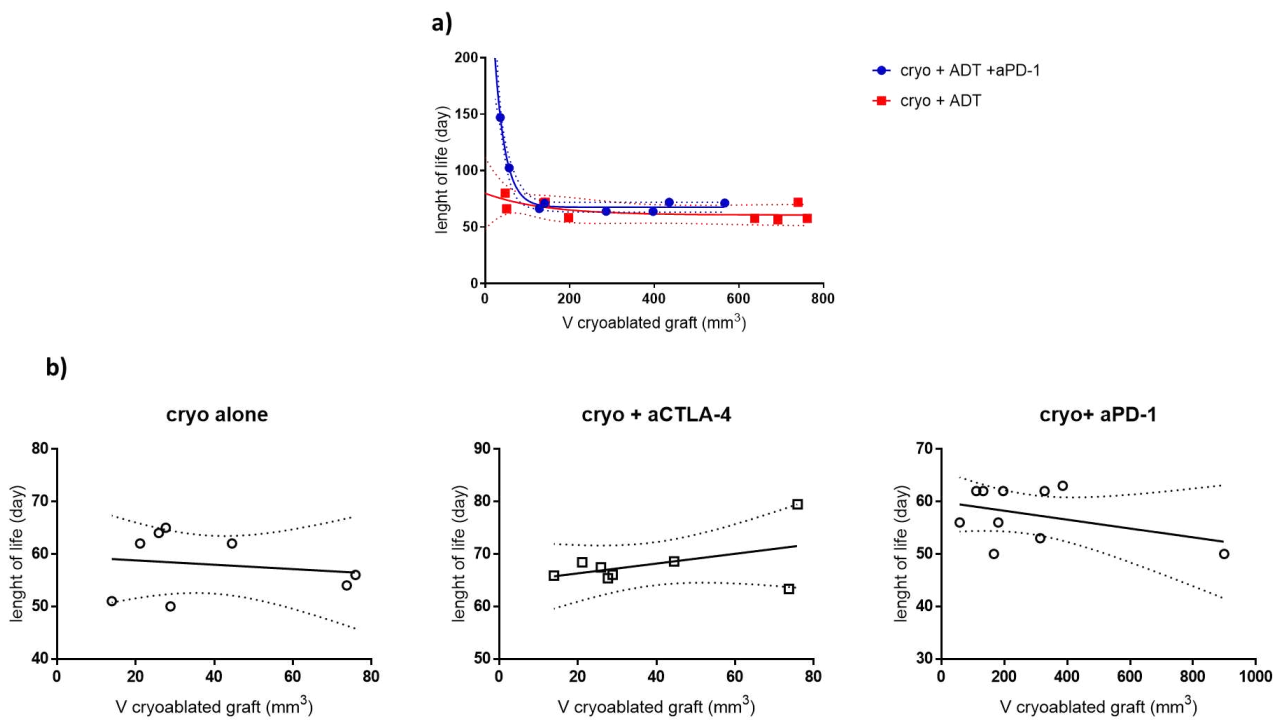
Figure 14. Relationship between mass of cryoablated tumor and lifespan. a) Therapeutic efficiency of best ADT based therapies decays exponentially with volume of cryoablated graft (R^2=98.7%, p=0.0131 for trimodal therapy and R^2=40%, p=0.07 for bimodal therapy). **b)** Other therapies do not show any associations between volume of cryoablated graft and lifespan (R^2=2.76%, p=0.696 for cryoablation alone; R^2=20.24%, p=0.2633 for cryoablation and anti CTLA-4 bimodal therapy; R^2=15.22%, p=0.2605 for cryoablation and anti PD-1 treatment).

Characterization of Immune Response

Systemic, regional and local immune responses could be crucial for the development of anti-cancer immunity (86). Accordingly, we performed flow cytometric analyses on the spleen, tumor d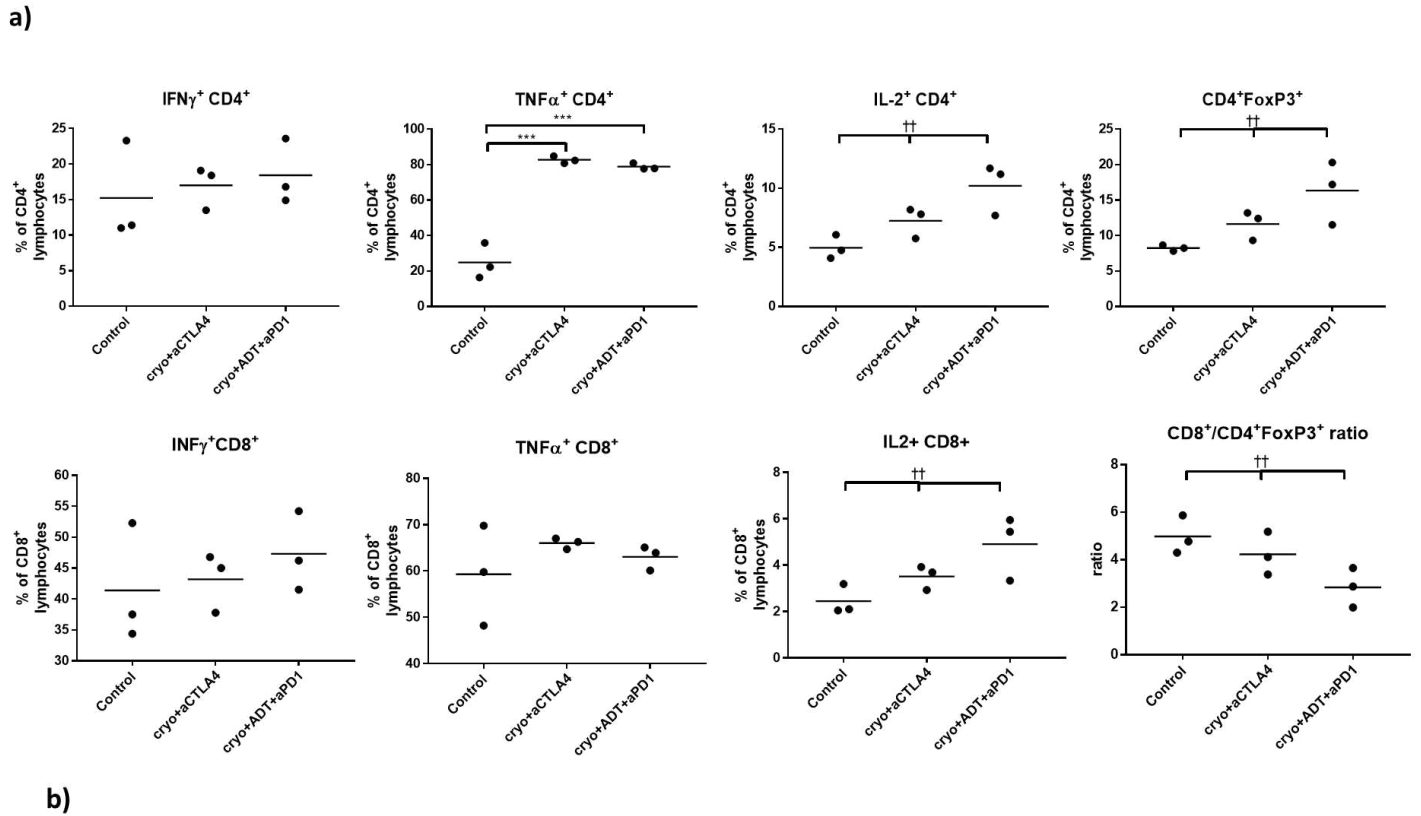raining lymph node of the distant, untreated tumor graft, and lymphocytes within the distant untreated tumor graft. Tissues were harvested 2 weeks after tumor cryoablation utilizing experimental groups that showed the most robust treatment effects. We examined activation of CD4$^+$ and CD8$^+$ cells in the spleen by examining secretion of IFNγ, TNFα and IL-2 (Figure 15a). Mice treated with trimodal therapy showed an average increase of 13.8% (95% CI 7.2-22.83, p=0.05) and 6.61% (95% CI 4.5-9.63, p=0.02) in CD8+IFNγ+ and CD4+IFNγ+ populations, respectively, when compared to control mice. Increased TNFα secretion was also noted in both CD4$^+$ and CD8$^+$ cells. Consistent with trimodal therapy, bimodal therapy with cryoablation and aCTLA-4 also caused an increase in TNFα$^+$ and IFNγ$^+$ populations. T regulatory cells (CD4$^+$FoxP3$^+$) were increased in bimodal and trimodal therapies by 3.49% (95% CI 2.03-4.45, p=0.01) and 3.5% (95% CI 2.13 – 4.92, p=0.02), respectively, when compared to control. Interestingly, this change did not reflect an alteration in the CD8/Treg ratio, which was equal in all experimental groups (Figure 15a). Next, we studied expression of immune checkpoint molecules in splenic lymphocytes (Figure 15b). Both bimodal and trimodal therapies demonstrated a decreased expression of PD-1 on CD8$^+$ lymphocytes by 9.7% (95% CI 6.9-13.03, p=0.008) and 14.63% (95% CI 12.26-18.13, p=0.001), respectively. Similar changes were noted also on CD4$^+$ cells. Expression of Lag-3 and Tim-3 on CD8$^+$ and CD4$^+$ cells was also significantly reduced in both therapeutic groups when compared to control.

Changes in remaining tumor graft draining lymph node in general paralleled those in spleen, however differences were smaller and not statistically significant with the exception of a reduction of expression of Lag-3 and Tim-3 on CD8$^+$ and CD4$^+$ cells when compared to controls. (Figure 16a, b). Unlike TNFα$^+$ CD4$^+$ cells which increased with therapeutic efficacy, CD8$^+$/Treg ratio decreased by the average of 0.9 (95% CI -1.7 to -0.17, p=0.0484) per therapeutic group (Figure 16a).

In trimodal therapy treated animals, the tumor graft had a 19-fold higher (95% CI 5.88 – 58, p=0.0001) lymphocyte infiltrate per mg of tumor when compared to control (Figure 17a). Among CD4$^+$ cells, treatment groups showed an increase in TNFα secretion with and a decrease in IFNγ secretion. The trimodal therapy group had a 13.9% (95% CI 8.8-17.2, p=0.0253) decrease in Treg cells when compared to control mice and had a 2.1 (95% CI 1.28 – 3.34, p=0.0143) increase in CD8/Treg ratio in comparison to control and bimodal therapy groups. Analyses of immune checkpoint expression (Figure 17b) following trimodal therapy demonstrated a 25% (95 CI% 9.97-37.47, p=0.04) decrease in Lag-3$^+$ CD4$^+$ cells when compared to control mice. The only significant difference between cryoablation and anti CTLA-4 treated mice compared to control mice was a 16% (95% CI 8.44 - 23.65, p=0.03) decrease in Tim-3$^+$ CD8$^+$ cells.

Figure 15. Characterization of immune response in spleens of most effective treatment groups. **a)** Cytokine profile of CD4^{+} and CD8^{+} lymphocytes. **b)** Expression of immune check point molecules on CD4^{+} and CD8^{+} lymphocytes. Data are presented as scatter plots with mean, each data point represents a sample made by combining 2 mice from same treatment group, means were compared by t test, significance of linear trend between means and treatment groups was tested by test for linear trend. *p<0.05, ** p<0.01, *** p<0.001 for t test; † p<0.05, †† p<0.01, ††† p<0.001, for test for linear trend*

a)

b)

Figure 16. Characterization of immune response in tumor draining lymph nodes of most effective treatment groups. **a)** Cytokine profile of CD4+ and CD8+ lymphocytes. **b)** Expression of immune check point molecules on CD4+ and CD8+ lymphocytes. Data are presented as scatter plots with mean, each data point represents a sample made by combining 2 mice from same treatment group, means were compared by t test, significance of linear trend between means and treatment groups was tested by test for linear trend. *p<0.05, ** p<0.01, *** p<0.001 for t test; † p<0.05, †† p<0.01, †††
p<0.001, for test for linear trend
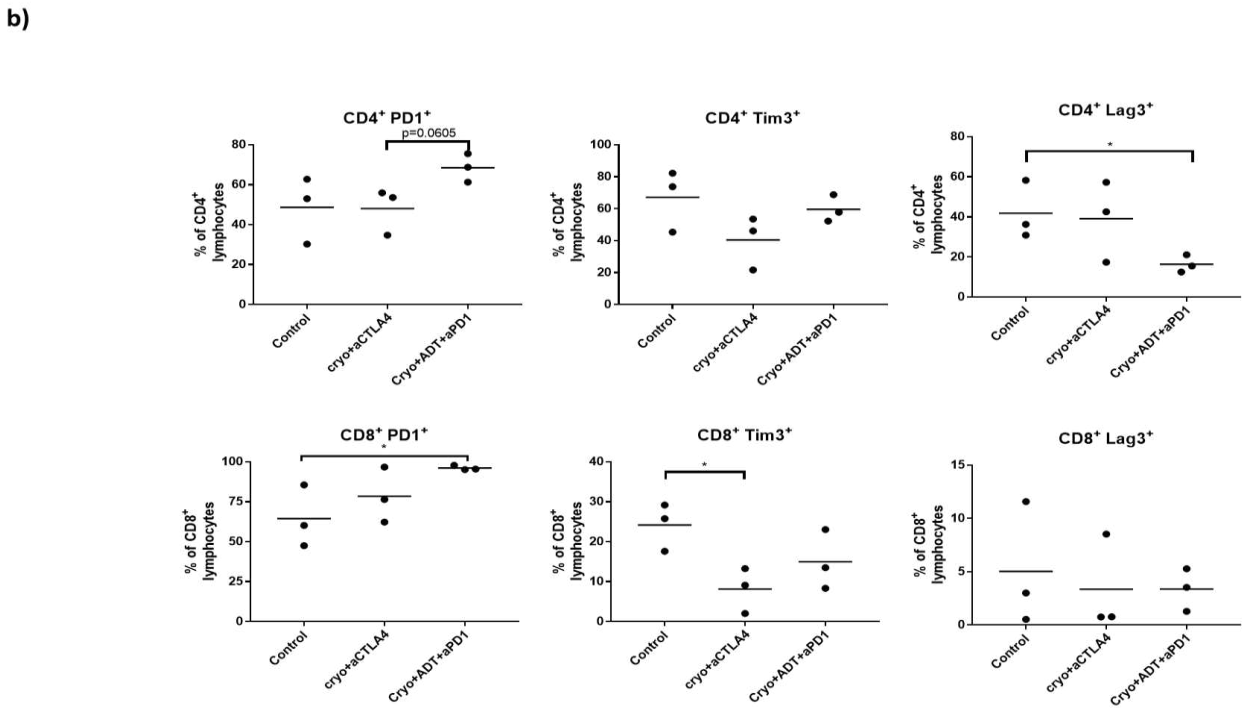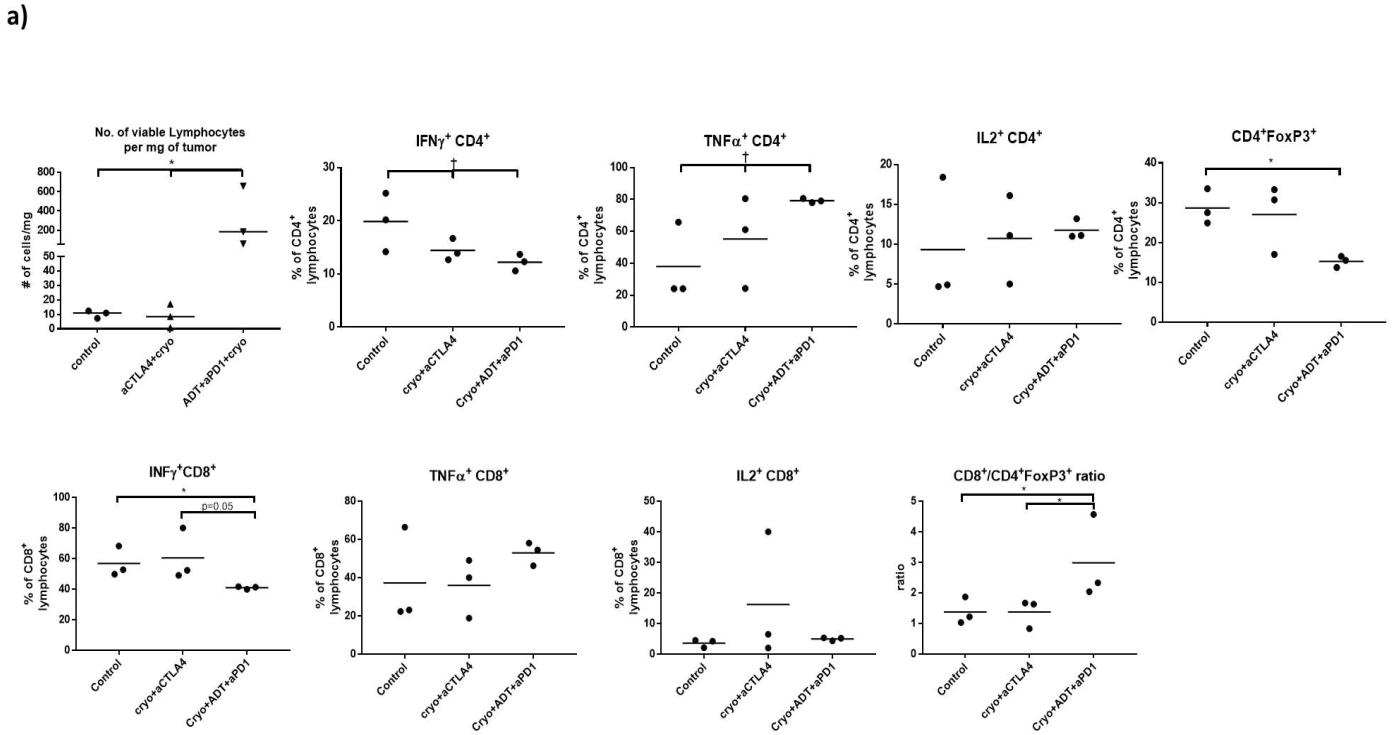
Figure 17. Characterization of immune response in remaining tumor grafts of most effective treatment groups. **a)** Cytokine profile of CD4$^+$ and CD8$^+$ lymphocytes. **b)** Expression of immune check point molecules on CD4$^+$ and CD8$^+$ lymphocytes. Data are presented as scatter plots with mean, each data point represents a sample made by combining 2 mice from same treatment group, means were compared by t test, significance of linear trend between means and treatment groups was tested by test for linear trend. *$p<0.05$, ** $p<0.01$, *** $p<0.001$ for t test; † $p<0.05$, †† $p<0.01$, ††† $p<0.001$, for test for linear trend*

Epigenetic modifiers do not add any benefit to ADT, cryoablation and anti-PD-1 trimodal therapy

Based on Kim et al. (66) we hypothesized that epigenetic modifiers 5 azacytidine (5AZA) and entinostat (ENT) can improve systemic immune response against remaining tumor isograft (Figure 18a). Adding 5AZA and ENT to ADT and anti-PD-1 reduced mortality rate by the factor of 3.3 (HR=0.3, 95% CI 0.09-0.94, p=0.03) when compared to ADT and anti-PD-1 combination. However, when 5AZA, ENT, ADT and anti-PD-1 therapy was compared to ADT monotherapy no survival benefit was observed (HR=0.79, 95% CI 0.28-2.25, p=0.67). None of these therapies delayed remaining graft growth thus pointing to the delay of larger graft growth as a primary mechanism for prolongation of lifespan (Figure 18d).

When compared to cryoablation and anti-PD-1 bimodal therapy addition of epigenetic modifiers decreased mortality rate almost five-fold (HR=0.22, 95% CI 0.068-0.742, p=0.02) (Figure 18b). This was accompanied by remaining graft delay of 5.24 days (95% CI 1.3-8.7, p=0.007) on average (Figure 18d). Also, when compared to cryoablation alone addition of epigenetic modifiers caused similar benefit in mortality reduction (HR=0.24, 95% CI 0.07-0.79, p=0.01) (Figure 18b).

Finally, we tested for synergy between epigenetic modifiers and trimodal therapy. 5AZA and ENT did not improve survival when compared to trimodal therapy (HR=1.25, 95% CI 0.46-3.38, p=0.65). Furthermore, epigenetic modifiers did not increase the number of long term surviving mice (Figure 18c, d).

In addition to these results mice treated with epigenetic modifiers showed clinical signs of distress and experienced one treatment related death.

Surgery (excision) and radiation synergize with low dose anti-CTLA-4 treatment

As expected, when compared to control group surgery monotherapy decreased mortality rates by the factor of 4 (HR=0.22, 95% CI 0.07-0.77, p=0.01) (Figure 19a). Surgery alone did not delay remaining tumor fast growth phase when compared to control mice (Figure 19c). Combining surgery with CTLA-4 blockade caused 7-fold mortality rate decrease

(HR=0.13, 95% CI 0.03-0.50, p=0.002) and 17.2 (95% CI 9.13 -25.16, p=0.0003) days delay of fast tumor growth in comparison to surgery monotherapy (Figure 19a, c).

Single dose 10 Gy irradiation of larger tumor graft delayed fast growth phase of remaining grafts for 4.1 (95% CI 0.45-7.41, p=0.02) days and decreased mortality rate almost 5-fold (HR=0.2, 95%CI 0.06-0.71, p=0.008) when compared to control mice (Figure 19a, c). Adding anti-CTLA-4 antibodies to radiation improved survival rates by almost 3-fold (HR=0.38, 95% CI 0.12-1, p=0.02) and delayed remaining tumor growth by 12.3 (95% CI 9.95-18.56, p=0.0006) days (Figure 19a, c).

Surgery (excision) and radiation do not synergize with anti-PD-1 treatment

Anti-PD-1 combination with surgery and did not show any synergy in terms of survival benefit (HR=0.93, 95% CI 0.36-2.37, p=0.87) nor in remaining tumor graft growth delay (median difference=5.54, 95% CI -1.39 to 12.1, p=0.1) when compared to surgery alone. Single dose radiation also did not demonstrate any synergistic effect with anti-PD-1 treatment (HR=0.74, 95% CI 0.22-1.82, p=0.65; median remaining graft growth delay= 0.57, 95% CI -4.89 to 4.95, p=0.95) when compared to radiation monotherapy (Figure 19b, c).

Next, we tried to capitalize on findings from Dewan et al. and combine PD-1 blockade and fractionated radiation (3x 3.3 Gy). However, fractionated radiation did not show any benefit when compared to single dose radiation nor has it demonstrated a synergism with aPD1 when compared either to single or fractionated dose radiation (Figure 20).

Surgery (excision) or single dose radiation do synergize with neoadjuvant ADT and anti-PD-1 blockade

In comparison to trimodal therapy with cryoablation, ADT and anti-PD-1 surgery in combination with ADT and anti-PD-1 did not cause any long-term survival in mice, furthermore when survival of all mice in groups was compared no extra benefit was shown (HR=1.8, 95% CI 0.61-5.37, p=0.35). Also, similar patterns of differences were noted in tumor growth delay analysis (Figure 21).

Single dose radiation similarly to surgery demonstrated no additional benefit in terms of remaining graft growth delay and survival when compared to cryoablation based trimodal therapy.
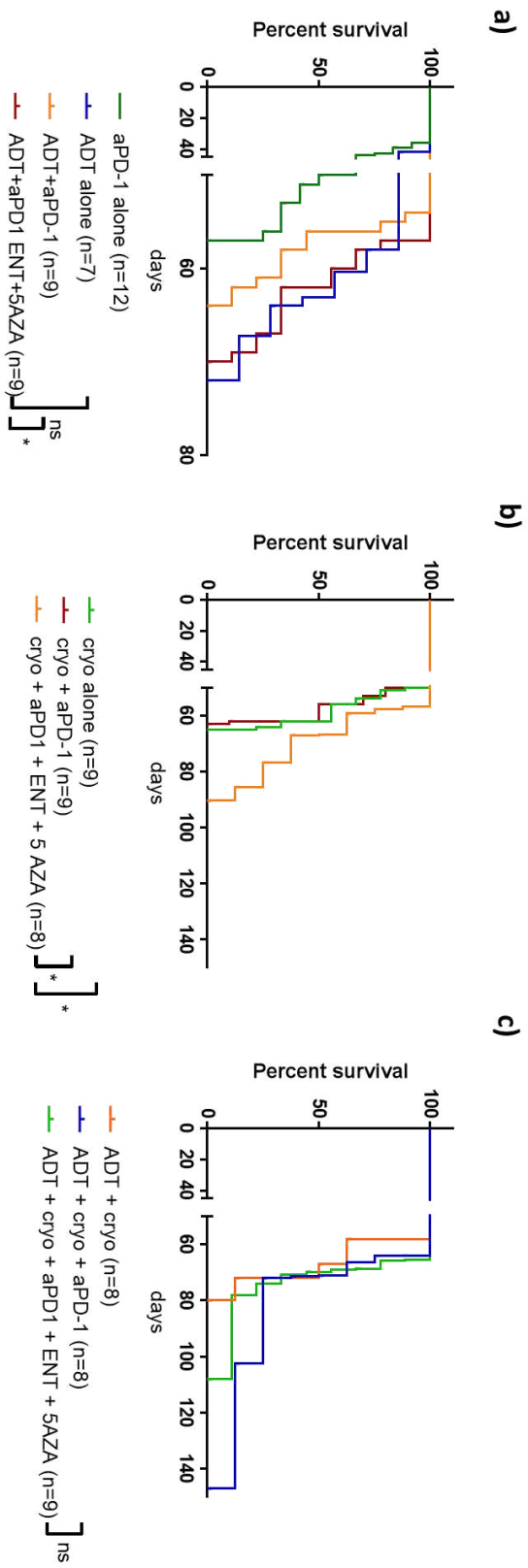
Figure 18. Effects of epigenetic modifiers on cryoablation and anti-PD-1 based treatments in terms of survival **(a, b, c)** and remaining tumor growth delay **(d)**. * *p<0.05,* ** *p<0.01,* *** *p<0.001*

d)

54
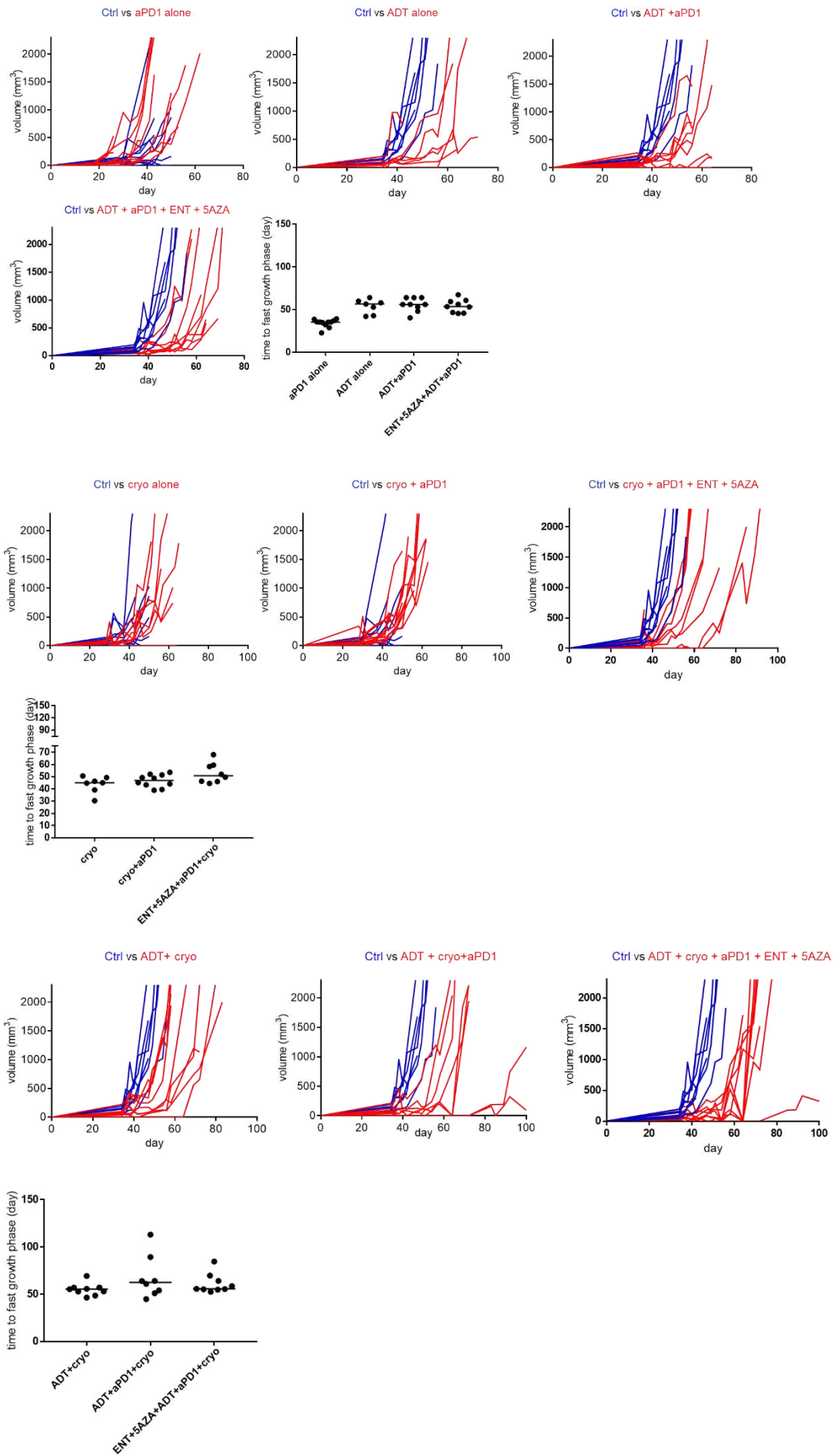
a)
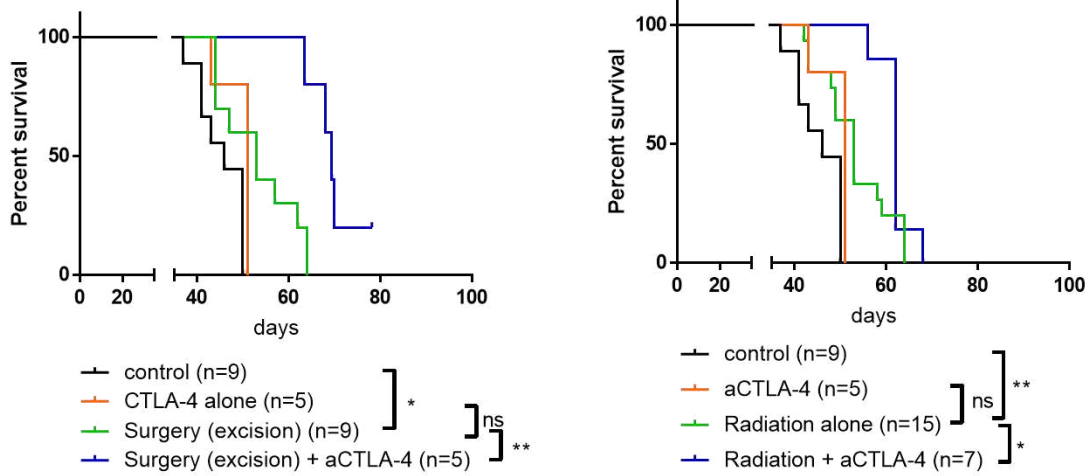
b)
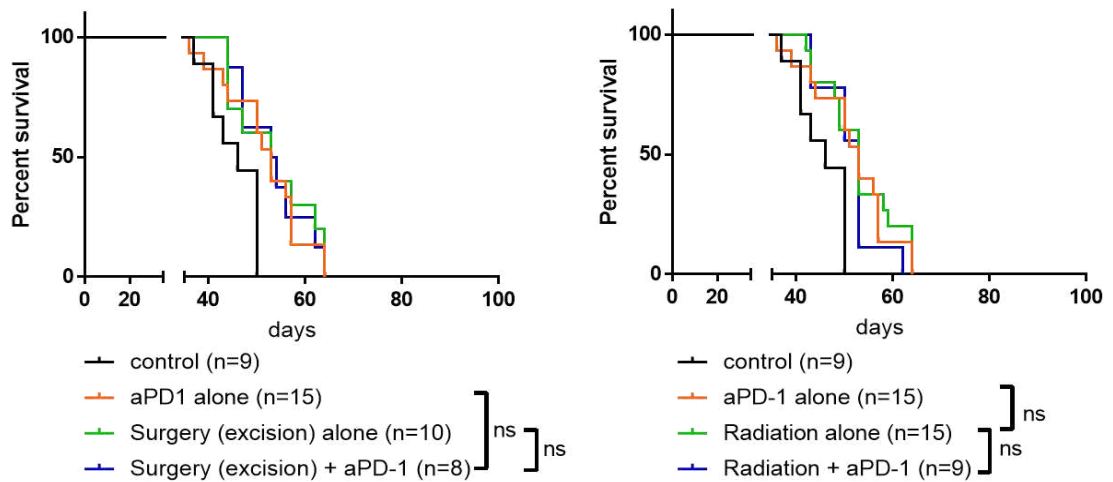
Figure 19. a, b, c) Survival and growth curves of mice treated with surgery or radiation-based therapies. *p<0.05, ** p<0.01, *** p<0.001*

c)

56
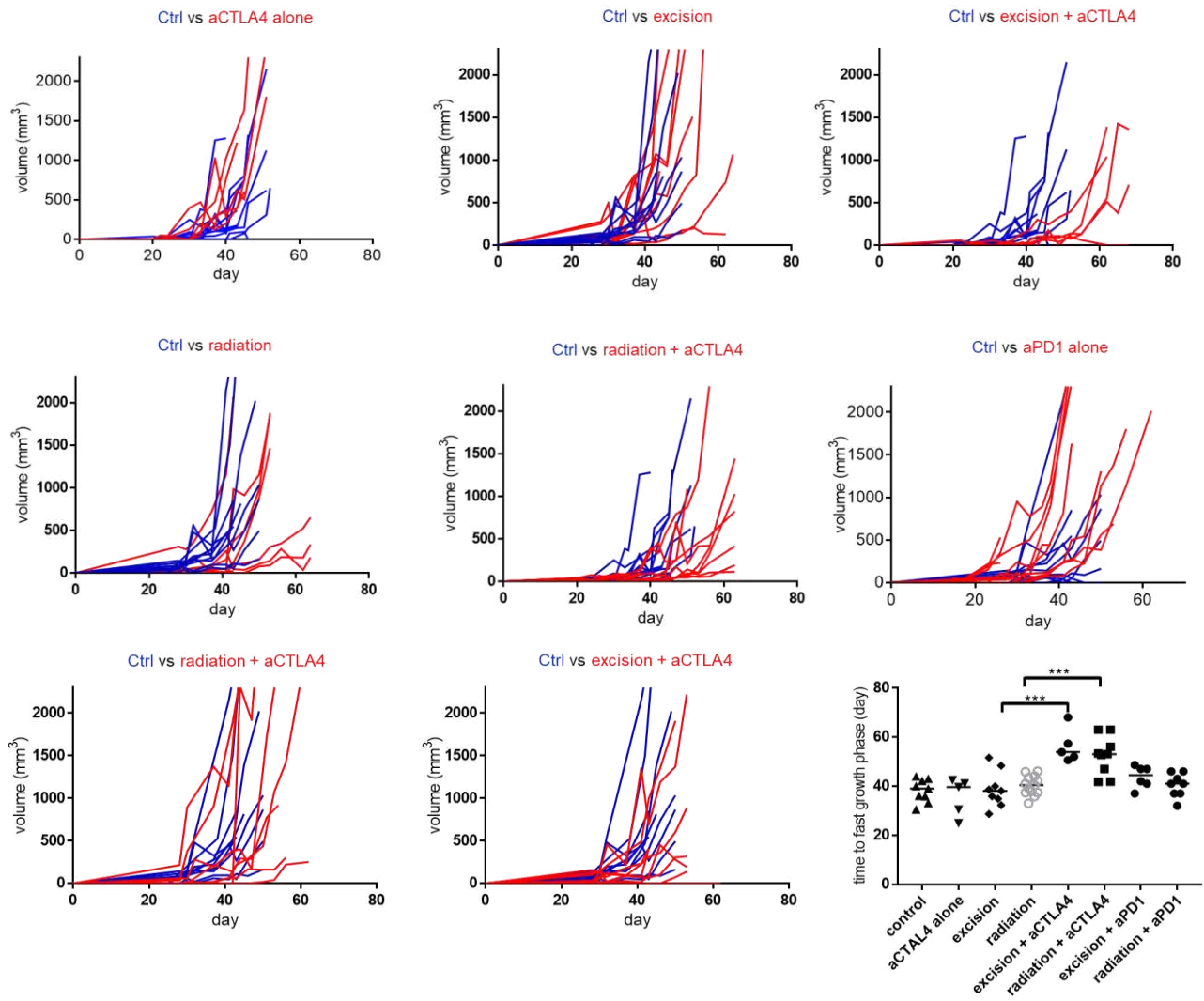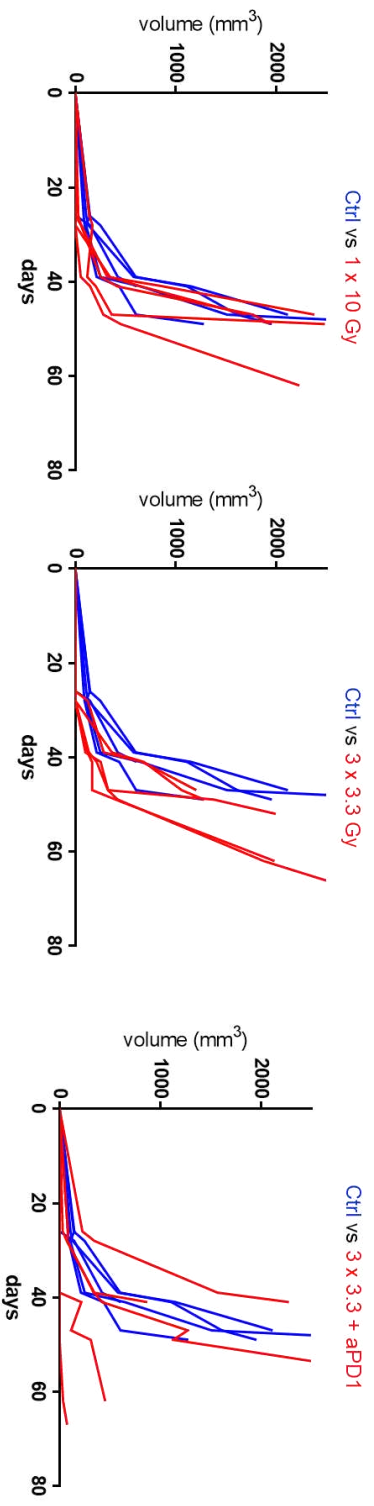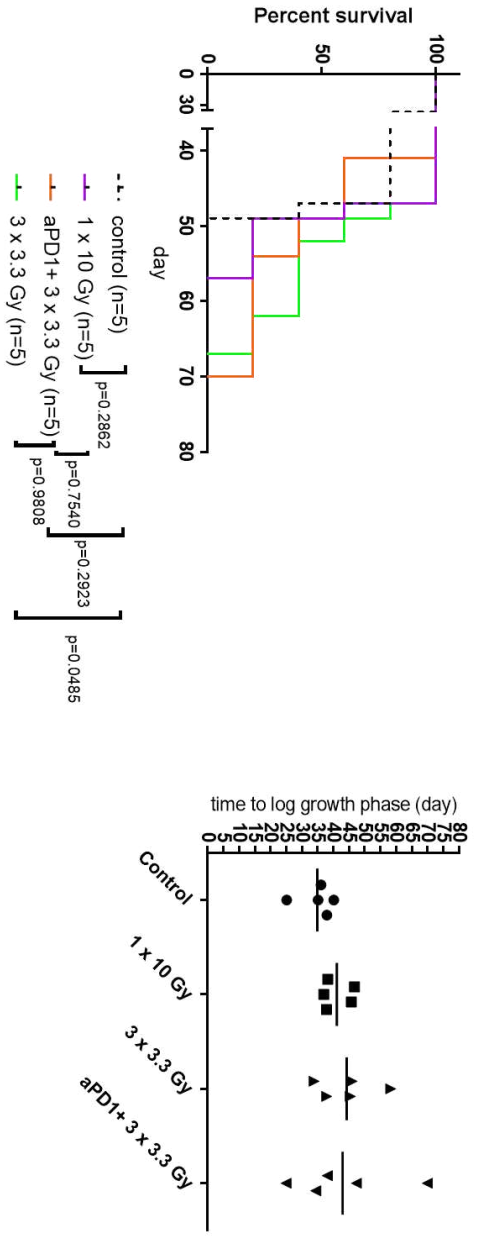
Figure 20. Effects of fractionated radiation on anti-PD-1 therapy.
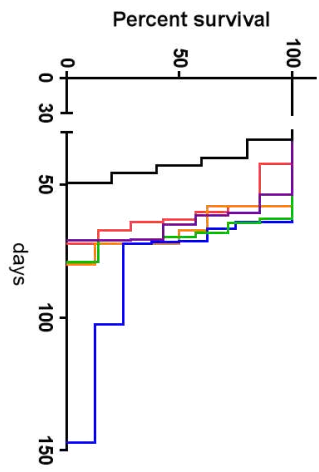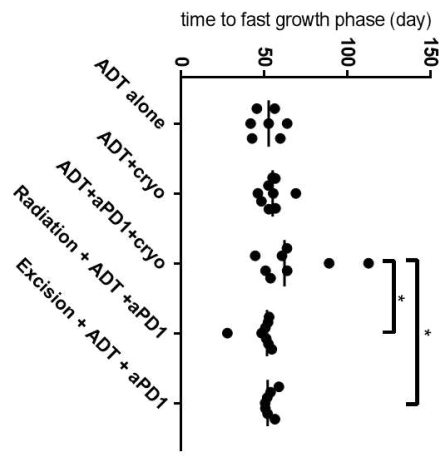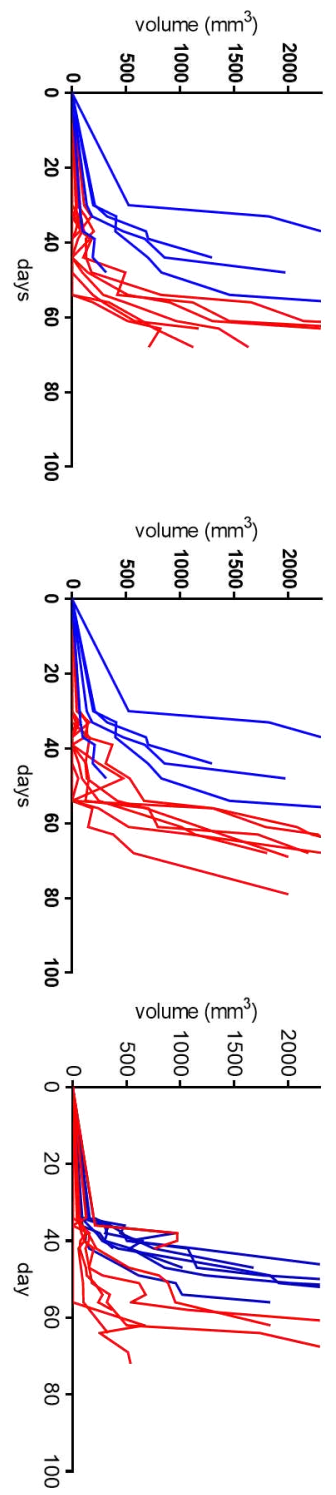
Figure 21. Growth curves and survival of surgery (excision) and radiation based trimodal therapies.

*p<0.05, ** p<0.01, *** p<0.001 for F test for variances*

58

Discussion

Discussion of "Characterization of Prostate Cancer Immune Microenvironment" Study

Recent successes in the treatment of melanoma, bladder, lung and other malignancies with checkpoint blockade has galvanized efforts to understand the interplay between tumors and the immune system and to develop novel therapeutic strategies in immuno-oncology (87-89). While immunotherapies have demonstrated efficacy in prostate cancer, to date, their benefit has been somewhat marginal (56, 57). B7-H3, is an attractive target for further study in prostate cancer based on immuno-histochemical data suggesting its increased levels in aggressive and castrate resistant metastatic prostate cancer and its homology to PD-L1 suggesting a potential role in immune modulation (90-93). Indeed, recently reported phase I results with Enoblituzumab (MGA271), a Fc-optimized monoclonal antibody targeting B7-H3 have shown signs of singe agent activity in advanced malignancies including prostate cancer (94). Here we examine B7-H3 at the level of gene expression and perform exploratory analyses to generate hypotheses regarding its relationship to the androgen axis and immune regulatory pathways in prostate cancer.

We found that B7-H3 was expressed in the majority of patients with localized prostate cancer. This was in contrast to PD-L1, PD-L2 and B7-H4, all of which showed low levels of expression and parallels findings of B7-H3 and other B7 homologs studied at the protein level. Similar to what is found in immunohistochemical studies, B7-H3 expression was associated with higher grade and stage disease, castrate resistant prostate cancer, and disease progression after local treatment. Our data thus supports the increased expression of B7-H3 in aggressive disease and suggests that RNA expression levels of B7-H3 may act as a good surrogate for protein level expression.

B7-H3 expression was strongly correlated with ERG positivity and negatively correlated with triple negative tumors. This suggested a putative relationship between B7-H3 and androgen signaling, which was reinforced by gene set enrichment of androgen receptor signaling and correlation of B7-H3 expression with the androgen receptor. In addition, a possible androgen response element was identified in the 5' UTR of B7-H3, with occupancy being dependent on the presence of androgens. Taken together, this data suggests that B7-H3 expression is regulated by the androgen signaling axis.

Whether B7-H3 plays a pro-inflammatory or immuno-suppressive role in human prostate cancer remains unclear. An examination of B7-H3 expression in relation to other immune pathways and genes suggested an association with TGF-beta signaling. Further, a positive correlation with RORC, FoxP3 and IL17 may be suggestive of increased B7-H3 being related to a Th17 type response (as seen in animal models) and possibly with an increase in Tregs (95). It is also worth noting that a number of animal studies suggest that B7-H3 has a stimulatory role in driving anti-tumor immunity, such that, contrary to the findings presented here—increased B7-H3 expression might be expected to correlate with improved clinical outcome. Indeed, studies of forced expression in a lymphoma model (96), a mastocytoma model (97) and a colorectal cancer model (98) suggest that B7-H3 interacts with a stimulatory receptor on CD8 T cells, and that this receptor may be TLT-2 (99). Data in certain human cancers are consistent with an anti-tumor role for B7-H3; in both gastric (100) and pancreatic cancer (101) expression is associated with improved survival. In other human cancers such as renal cell carcinoma (102) and prostate cancer ((92) and data shown here), B7-H3 expression is associated with a poor outcome. The reasons for this apparent discrepancy are not immediately obvious but could potentially be explained by differential expression of activating versus inhibitory B7-H3 receptors on immune cells, or by differential infiltration of tumor subtypes with sets of immune cells. For example, expression of a stimulatory B7-H3 receptor on pro-tumor M2 macrophages or myeloid derived suppressor cells could occur in tumors in which B7-H3 expression is associated with poor outcome— here the stimulation of suppressive cells could lead to tumor progression. Conversely, in another tumor types the B7-H3 receptor could be expressed predominantly on tumor specific CD8 T cells, so that receptor engagement could lead to an anti-tumor effect, as has been observed in most animal studies. This dual effect is not specific to B7-H3, infiltration of tumors with regulatory T cells is associated with poor outcome in most tumors, (103) but not in colorectal cancer, where it is associated with an improved outcome (104). Identification of the human B7-H3 receptor(s) would provide crucial insights in terms of resolving these issues.

As B7-H3 directed therapy enters into clinical study in human prostate cancer it will be critical to perform correlative science to help tease out which molecular interactions can be capitalized on, particularly for combination therapy trials.

In summary, we find that B7-H3 expression is present in the majority of prostate cancer cases, with levels of B7-H3 increasing with tumor extent and aggressiveness. B7-H3 is potentially androgen regulated and related to the TGF-beta signaling pathway, however these associations need further study. B7-H3 expression characteristics may help guide patient selection for clinical trials.

Discussion of Improving Immune Check Point Blockade in Metastatic Prostate Cancer Treatment Study

Developing novel approaches for the treatment of advanced prostate cancer is of paramount importance. The combination of local therapies and immune-checkpoint blockade could potentially increase the efficacy of treatment at distant tumor sites. Here we utilized a straightforward mouse model with which to assess potential abscopal effects in prostate cancer. We further demonstrate a possible T cell dependent synergy between cryoablation and checkpoint blockade in eliciting distant tumor responses. We find that oncological responses were uniform and not dependent on additional therapy when cryoablation was combined with anti-CTLA-4 therapy, and only effected a subset of the population and required neoadjuvant hormonal deprivation when cryoablation was combined with PD-1.

Previous animal models in which immune therapy of prostate cancer was assessed utilized an immune re-challenge design, and models that were not representative of prostate adenocarcinoma or tumor models engineered to have dominant artificial antigen (62, 105, 106). Synchronous tumor model such as ours have been tested in stetting of studying abscopal effect in breast cancer(55). Although we did not use heat ablation by high frequency ultrasound we think that it might also harbor a potential for eliciting an abscopal effect.

Anti-CTLA-4 and anti-PD1 or PDL1 treatments represent the most heavily studied checkpoint directed immunotherapies (107, 108). It is important to note that these immune checkpoints are functionally and spatially distinct (108). The CTLA-4/B7 checkpoint functions at secondary lymphoid organs and regulates the amplitude of early activation of naïve T cells during the immune response. This is in contrast to the PD-1/PDL1/2 checkpoint, which operates in the tissue micro-environment and limits the activity of T cells in peripheral organs. These differences not only influence the efficacy of treatment with checkpoint blockade, but also influence differences in the toxicity profiles of these molecules (with CTLA-4 having a less favorable toxicity profile) (109). The mechanistic differences of these therapies may explain our findings.

In mice treated with low-dose anti-CTLA-4 therapy, we found a uniform synergy of checkpoint blockade and cryotherapy. This result was abrogated by T cell depletion. In addition, T cell depleted mice treated with cryo-ablation and anti-CTLA4 therapy demonstrated survival and non-cryoablated tumor growths that were comparable to completely untreated control mice, suggesting a possible immunomodulatory role of cryoablation (as opposed to a result of simple decreased tumor burden). Combination of low dose anti-CTLA-4 and cryoablation was accompanied by increased activation of splenic T cells along with lower expression of other immune checkpoint molecules. However, the local tumor immune response was comparable to control mice regarding to the number of tumor infiltrating lymphocytes (TILs), the CD8+ cell cytokine profiles, and the CD8+/Treg ratio. Despite, these mice had the lowest expression of Tim-3 on CD8+ cells. Since flow cytometry analyses were performed at a single time point, further characterization of tumor infiltrating lymphocytes at additional timepoints might yield valuable insights into the intratumoral immune response.

In mice treated with anti-PD1 therapy, ADT was required to see an oncological benefit, and as stated, only a quarter of mice had prolonged survival or delayed untreated tumor growth. ADT has been previously shown to cause a T cell infiltrate and to modulate the immune response in both anti and pro-inflammatory sense (67, 83, 84, 110-112). Consistent with this, neoadjuvant ADT followed by cryoablation and PD-1 blockade increased systemic T cell activation in the spleen and markedly increased tumor infiltrating lymphocytes with favorable profiles including CD4+ TNFα secretion and the CD8+/Treg ratio when compared to control and low dose anti-CTLA-4 based bi-modal therapy. While degarelix, a GnRH antagonist, has not been widely investigated in the context of immunotherapy, our data and the work of others (112) support that it functions similarly to GnRH agonists in immune based treatment regimes. Since the oncologic benefit occurred in only a fraction of the treated mice, we hypothesize that neoadjuvant degarelix treatment may have acted as an inconsistently efficacious priming agent for the T cell dependent responses seen. Furthermore, such partial response were negatively corelated with masses of cryoablated tumor pointing out to the immune supression due to extensive tissue injury.

In order to compare all therapies a decision theoretic principle of maximizing utility in terms of immunogenicity measure, i.e. time to fast growth of remaining tumor graft, and

minimizing the risk in terms of observed side effects was used. We informally compared

different therapies by their medians and interquartile range (Figure 22).
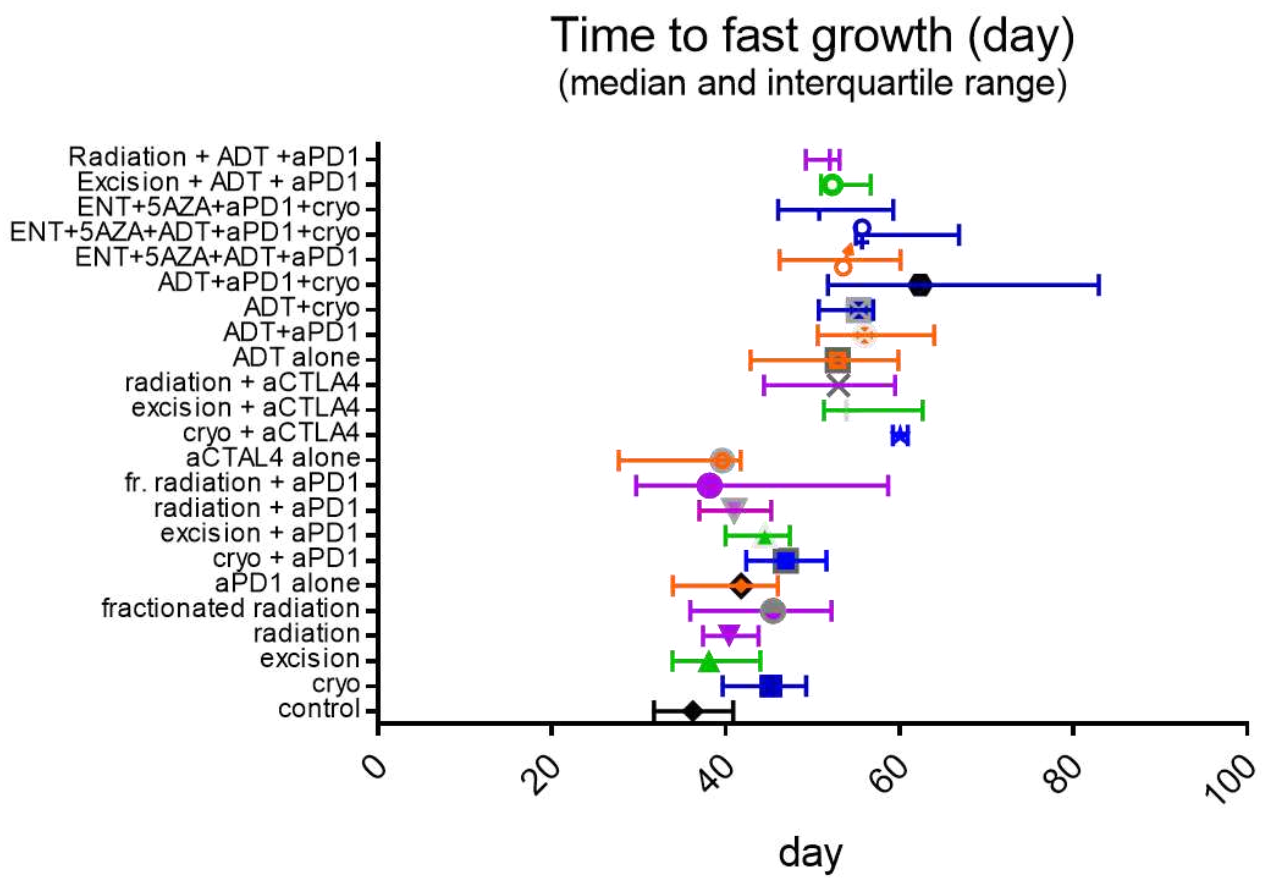
Figure 22. Comparison of all therapeutic groups

Maximum delays in onset of fast growth phase were observed in mice treated with neoadjuvant ADT, cryoablation and PD-1 blockade combination. These mice also did not show any signs of side effects. Furthermore, one dose of ADT makes this therapeutic option attractive in terms of translation to patients because it minimizes chances for the development of androgen resistance. Radiation-based therapies did not show any extra therapeutic gain when compared to cryoablation based regimes. Nevertheless, we still think that external beam radiation might harbor therapeutic potential since single 10Gy dose never completely ablated the larger graft what impacted the survival rates negatively and might have caused additional impairment of anti-tumor immunity.

Regardless, encouraged by the findings in this study, we have developed an ongoing phase II clinical trial of cryoablation combined with anti-PD-1 therapy and androgen deprivation in men with oligometastatic hormone naïve prostate cancer (NCT02489357).

There are many limitations to our study and areas which will benefit from further investigation. Among these is that we only studied complete tumor ablation as a method to elicit a distant immune response and were not able to investigate the immune response within the ablated graft or distant graft at multiple time points. It is possible that methodologies employing partial ablation of tumors might have resulted in a greater immune-oncological effect in distant tumors (85). Further, examination of tumor infiltrating lymphocytes at multiple time points might have provided more insight into the nature of the immune mediated effect. In addition, we employed treatment regimens with check point blockade administered both before, during and after treatment with the intent of mitigating pre-existing immune suppression, boosting T cell activation upon antigen presentation and then allowing for T cell activation and expansion (113, 114). It is possible that treatment with checkpoint blockade at all of these time points is not necessary or, conversely, that longer duration of checkpoint blockade would have allowed for a more complete response in experimental arms treated with anti-PD1 based therapy.

Results from immunotherapy trials in prostate cancer have not been as favorable as those seen in other malignancies, suggesting that effective immunotherapy in prostate cancer will likely require a multi-modal approach. Use of local therapies may be able to boost an anti-neoplastic immune response in prostate cancer, but may require additional adjuncts to treatment, particularly when using anti-PD1 based therapeutics. As optimization

of combinatorial approaches to immunotherapy require study not only of which therapies best synergize but also their optimal dosing and timing of administration (113, 114), immuno-competent animal models will be critical for the better design and outcomes of human trials.

Conclusion

B7-H3 is associated with negative oncological outcomes in prostate cancer. B7-H3 is regulated by androgen signaling pathways, gene ontology analysis showed that it might be involved in TGF-β signaling and Th17 inflammatory response.

Cryoablation synergizes with low dose (1mg/kg) anti-CTLA-4 treatment, PD-1 blockade needs to be combined with neoadjuvant ADT and cryoablation in order to be effective. Such trimodal therapy despite being effective in 25% of animals yielded the overall longest surviving mice.

Abstract

Objective: To screen for possible therapeutic targets in prostate cancer immune microenvironment and to test if some of local ablative therapies can elicit abscopal effect in conjunction with immune check point blockade.

Patients, Methods and Materials: 3 patients cohorts were used to identify potential therapeutic targets and to reconstruct their interactome. Association between candidate genes and oncological outcomes were established using the Kaplan Maier analysis and logistic regression.

To test the abscopal effect FVB/NJ mice were injected subcutaneously into each flank with either $1 \cdot 10^6$ or $0.2 \cdot 10^6$ isogenic hormone sensitive Myc-Cap cells to establish synchronous grafts. Mice were treated with four intraperitoneal injections of anti-PD-1 (10mg/kg), anti-CTLA-4 (1mg/kg), or isotype control antibody with or without adjuvant ablation of the larger tumor graft and with or without neo-adjuvant androgen deprivation with degarelix (ADT). Mouse survival and growth rates of tumor grafts were measured.

Results: B7-H3 expression was present in the majority of localized prostate cancer cases and was positively associated with Gleason score (p<0.001), tumor stage (p <0.02), and castrate resistant metastatic disease (p<0.0001). Within prostatectomy tissue, high B7-H3 expression correlated with the development of metastasis and prostate cancer specific mortality, but this was not significant on multi-variable analysis. B7-H3 expression correlated with ERG+ disease (r = 0.99) and AR expression (r=0.36). ChIP analysis revealed AR binding upstream of B7-H3, suggesting potential androgen dependent regulation. Gene set enrichment analysis also demonstrated an association of B7-H3 with androgen signaling as well as immune regulatory pathways.

Treatment with anti-CTLA-4 antibody and cryoablation delayed the growth of the distant tumor by 14.8 days (p=0.0006) and decreased the mortality rate by factor of 4 (p=0.0003) when compared to cryoablation alone. Combining PD-1 blockade with cryoablation did not show a benefit over use of either treatment alone. Addition of ADT to anti-PD1 therapy and cryoablation doubled the time to accelerated growth in the untreated tumors (p=0.0021) and extended survival when compared to cryoablation combined with ADT in 25% of the mice. Effects of combining anti-PD1 with ADT and cryoablation on mouse survival were obviated by T cell depletion.

Conclusion: B7-H3 expression correlates with high Gleason grade and advanced prostate cancer stage with higher expression portending poor oncologic outcomes in prostatectomy cohorts. B7-H3 expression appears to related to androgen signaling as well as the immune reactome.

68

Trimodal therapy consisting of androgen deprivation, cryoablation and PD-1 blockade as well as the combination of cryoablation and low dose anti-CTLA-4 blockade showed that local therapies with cryoablation could be considered to augment the effects of checkpoint blockade in prostate cancer.

Sažetak

Ciljevi: Pretražiti imunološki mikro-okoliš na potencijalne terapijske mete i pokušati ostvari sustavni odgovor na rak prostate pomoću kombinacija lokalne ablacije i blokatora imunološke kontrolne točke

Ispitanici i tvoriva: 3 retrospektivne kohorte pacijenata su upotrjebljene kako bi se identificirale mete u imunološkom mikro-okolišu prostate i rekonstruirao njihov interaktom. Pri tom su upotrjebljene tehnike Kaplan Meirove analize i logističke regresije.

Kako bi se uspostavio životinjski model za testiranje sustavnog odgovora na rak prostate svakom mišu su usađena 2 usatka tumora prostate. Nakon 3 tjedana veći usadak je ablatiran te su primijenjeni blokatori imunološke kontrolne točke. Preživljenje i odgoda rasta tumora su bile glavne mjere ishoda.

Rezultati: Identificiran je samo jedan gen (*B7-H3*) kao moguća meta, pokazalo se da je pod regulacijom signalnih puteva androgena te da postoji mogućnost njegovog sudjelovanja u upalnom odgovoru.

Krijoablacija i blokada CTLA-4 (1mg/kg) su pokazali sinergijski učinak odgađajući rast ostatnog tumora za 14.6 (p=0,0006) dana u usporedbi s samom krioablacijom. Da bi kombinacija blokade PD-1 (10 mg/kg) i krijoablacije bila učinkovita mora joj se pridružiti neoadjuvantna anti-androgena terapija, tada u 25% slučajeva udvostručava preživljenje (p=0,0021) u usporedbi s kombinacijom krijoablacije i antiandrogena. Ostale ablativne terapije ne donose nikakvu dodatnu korist kada se usporede s krioablacijom.

Zaključak: *B7-H3* predstavlja potencijalnu terapijsku metu, reguliran je androgenima te postoji mogućnost da sudjeluje u upali. Trimodalna terapija krioablacijom, blokadom PD-1 i anti-androgenima u 25% slučajeva podvostručava životni vijek pokusnih životinja.

References

1. Siegel R, Naishadham D, Jemal A. Cancer statistics, 2013. CA Cancer J Clin. 2013;63(1):11-30.

2. Antonarakis ES, Armstrong AJ. Emerging therapeutic approaches in the management of metastatic castration-resistant prostate cancer. Prostate Cancer Prostatic Dis. 2011;14(3):206-18.

3. Katzenwadel A, Wolf P. Androgen deprivation of prostate cancer: Leading to a therapeutic dead end. Cancer Lett. 2015;367(1):12-7.

4. Cai C, He HH, Chen S, Coleman I, Wang H, Fang Z, et al. Androgen receptor gene expression in prostate cancer is directly suppressed by the androgen receptor through recruitment of lysine-specific demethylase 1. Cancer Cell. 2011;20(4):457-71.

5. Karantanos T, Evans CP, Tombal B, Thompson TC, Montironi R, Isaacs WB. Understanding the mechanisms of androgen deprivation resistance in prostate cancer at the molecular level. Eur Urol. 2015;67(3):470-9.

6. Network. NCC. Clinical practice gudelines in Oncology, Prostate cancer (Version 2.2018) 2018 [Available from: https://www.nccn.org/professionals/physician_gls/pdf/prostate.pdf.

7. Antonarakis ES, Lu C, Wang H, Luber B, Nakazawa M, Roeser JC, et al. AR-V7 and resistance to enzalutamide and abiraterone in prostate cancer. N Engl J Med. 2014;371(11):1028-38.

8. James ND, de Bono JS, Spears MR, Clarke NW, Mason MD, Dearnaley DP, et al. Abiraterone for Prostate Cancer Not Previously Treated with Hormone Therapy. N Engl J Med. 2017.

9. Bozic I, Reiter JG, Allen B, Antal T, Chatterjee K, Shah P, et al. Evolutionary dynamics of cancer in response to targeted combination therapy. Elife. 2013;2:e00747.

10. Nauts HC, McLaren JR. Coley toxins--the first century. Adv Exp Med Biol. 1990;267:483-500.

11. Hoption Cann SA, van Netten JP, van Netten C. Dr William Coley and tumour regression: a place in history or in the future. Postgrad Med J. 2003;79(938):672-80.

12. McCarthy EF. The toxins of William B. Coley and the treatment of bone and soft-tissue sarcomas. Iowa Orthop J. 2006;26:154-8.

13. L. G. Intradermal Immunization of C3H Mice against a Sarcoma That Originated in an Animal of the Same Line. Cancer Research. 1943.

14. Prehn RT. Analysis of antigenic heterogeneity within individual 3-methylcholanthrene-induced mouse sarcomas. J Natl Cancer Inst. 1970;45(5):1039-45.

15. Prehn RT. Relationship of tumor immunogenicity to concentration of the oncogen. J Natl Cancer Inst. 1975;55(1):189-90.

16.   Mitchison NA. Studies on the immunological response to foreign tumor transplants in the mouse. I. The role of lymph node cells in conferring immunity by adoptive transfer. J Exp Med. 1955;102(2):157-77.

17.   Fujimoto S, Greene MI, Sehon AH. Regulation of the immune response to tumor antigens. II. The nature of immunosuppressor cells in tumor-bearing hosts. J Immunol. 1976;116(3):800-6.

18.   Prehn RT. The immune reaction as a stimulator of tumor growth. Science. 1972;176(4031):170-1.

19.   Graham JB, Graham RM. The effect of vaccine on cancer patients. Surg Gynecol Obstet. 1959;109(2):131-8.

20.   Doherty PC, Zinkernagel RM. H-2 compatibility is required for T-cell-mediated lysis of target cells infected with lymphocytic choriomeningitis virus. J Exp Med. 1975;141(2):502-7.

21.   Steinman RM, Cohn ZA. Identification of a novel cell type in peripheral lymphoid organs of mice. I. Morphology, quantitation, tissue distribution. J Exp Med. 1973;137(5):1142-62.

22.   Herberman RB, Nunn ME, Holden HT, Lavrin DH. Natural cytotoxic reactivity of mouse lymphoid cells against syngeneic and allogeneic tumors. II. Characterization of effector cells. Int J Cancer. 1975;16(2):230-9.

23.   Herberman RB, Nunn ME, Lavrin DH. Natural cytotoxic reactivity of mouse lymphoid cells against syngeneic acid allogeneic tumors. I. Distribution of reactivity and specificity. Int J Cancer. 1975;16(2):216-29.

24.   Mier JW, Gallo RC. Purification and some characteristics of human T-cell growth factor from phytohemagglutinin-stimulated lymphocyte-conditioned media. Proc Natl Acad Sci U S A. 1980;77(10):6134-8.

25.   Lafferty KJ, Cunningham AJ. A new analysis of allogeneic interactions. Aust J Exp Biol Med Sci. 1975;53(1):27-42.

26.   Decker WK, da Silva RF, Sanabria MH, Angelo LS, Guimaraes F, Burt BM, et al. Cancer Immunotherapy: Historical Perspective of a Clinical Revolution and Emerging Preclinical Animal Models. Front Immunol. 2017;8:829.

27.   Rosenberg SA, Lotze MT, Muul LM, Leitman S, Chang AE, Ettinghausen SE, et al. Observations on the systemic administration of autologous lymphokine-activated killer cells and recombinant interleukin-2 to patients with metastatic cancer. N Engl J Med. 1985;313(23):1485-92.

28.   Rosenberg SA, Lotze MT, Muul LM, Chang AE, Avis FP, Leitman S, et al. A progress report on the treatment of 157 patients with advanced cancer using lymphokine-activated killer cells and interleukin-2 or high-dose interleukin-2 alone. N Engl J Med. 1987;316(15):889-97.

29.   Rosenberg SA, Packard BS, Aebersold PM, Solomon D, Topalian SL, Toy ST, et al. Use of tumor-infiltrating lymphocytes and interleukin-2 in the immunotherapy of patients with metastatic melanoma. A preliminary report. N Engl J Med. 1988;319(25):1676-80.

30.   Jonasch E, Haluska FG. Interferon in oncological practice: review of interferon biology, clinical applications, and toxicities. Oncologist. 2001;6(1):34-55.

31.   Herr HW, Morales A. History of bacillus Calmette-Guerin and bladder cancer: an immunotherapy success story. J Urol. 2008;179(1):53-6.

32.   Mueller DL, Jenkins MK, Schwartz RH. Clonal expansion versus functional clonal inactivation: a costimulatory signalling pathway determines the outcome of T cell antigen receptor occupancy. Annu Rev Immunol. 1989;7:445-80.

33.   Linsley PS, Brady W, Grosmaire L, Aruffo A, Damle NK, Ledbetter JA. Binding of the B cell activation antigen B7 to CD28 costimulates T cell proliferation and interleukin 2 mRNA accumulation. J Exp Med. 1991;173(3):721-30.

34.   Linsley PS, Brady W, Urnes M, Grosmaire LS, Damle NK, Ledbetter JA. CTLA-4 is a second receptor for the B cell activation antigen B7. J Exp Med. 1991;174(3):561-9.

35.   Krummel MF, Allison JP. CD28 and CTLA-4 have opposing effects on the response of T cells to stimulation. J Exp Med. 1995;182(2):459-65.

36.   Leach DR, Krummel MF, Allison JP. Enhancement of antitumor immunity by CTLA-4 blockade. Science. 1996;271(5256):1734-6.

37.   Bhatia S, Tykodi SS, Thompson JA. Treatment of metastatic melanoma: an overview. Oncology (Williston Park). 2009;23(6):488-96.

38.   Fuchs EJ, Matzinger P. Is cancer dangerous to the immune system? Semin Immunol. 1996;8(5):271-80.

39.   Demaria S, Ng B, Devitt ML, Babb JS, Kawashima N, Liebes L, et al. Ionizing radiation inhibition of distant untreated tumors (abscopal effect) is immune mediated. Int J Radiat Oncol Biol Phys. 2004;58(3):862-70.

40.   Okazaki T, Honjo T. PD-1 and PD-1 ligands: from discovery to clinical application. Int Immunol. 2007;19(7):813-24.

41.   Nizar S, Copier J, Meyer B, Bodman-Smith M, Galustian C, Kumar D, et al. T-regulatory cell modulation: the future of cancer immunotherapy? Br J Cancer. 2009;100(11):1697-703.

42.   Talmadge JE, Gabrilovich DI. History of myeloid-derived suppressor cells. Nat Rev Cancer. 2013;13(10):739-52.

43.   Korman AJ, Peggs KS, Allison JP. Checkpoint blockade in cancer immunotherapy. Adv Immunol. 2006;90:297-339.

44.	Maker AV, Phan GQ, Attia P, Yang JC, Sherry RM, Topalian SL, et al. Tumor regression and autoimmunity in patients treated with cytotoxic T lymphocyte-associated antigen 4 blockade and interleukin 2: a phase I/II study. Ann Surg Oncol. 2005;12(12):1005-16.

45.	Hodi FS, O'Day SJ, McDermott DF, Weber RW, Sosman JA, Haanen JB, et al. Improved survival with ipilimumab in patients with metastatic melanoma. N Engl J Med. 2010;363(8):711-23.

46.	Topalian SL, Hodi FS, Brahmer JR, Gettinger SN, Smith DC, McDermott DF, et al. Safety, activity, and immune correlates of anti-PD-1 antibody in cancer. N Engl J Med. 2012;366(26):2443-54.

47.	Reck M, Rodriguez-Abreu D, Robinson AG, Hui R, Csoszi T, Fulop A, et al. Pembrolizumab versus Chemotherapy for PD-L1-Positive Non-Small-Cell Lung Cancer. N Engl J Med. 2016;375(19):1823-33.

48.	Hamid O, Robert C, Daud A, Hodi FS, Hwu WJ, Kefford R, et al. Safety and tumor responses with lambrolizumab (anti-PD-1) in melanoma. N Engl J Med. 2013;369(2):134-44.

49.	Ferris RL, Blumenschein G, Jr., Fayette J, Guigay J, Colevas AD, Licitra L, et al. Nivolumab for Recurrent Squamous-Cell Carcinoma of the Head and Neck. N Engl J Med. 2016;375(19):1856-67.

50.	Cella D, Grunwald V, Nathan P, Doan J, Dastani H, Taylor F, et al. Quality of life in patients with advanced renal cell carcinoma given nivolumab versus everolimus in CheckMate 025: a randomised, open-label, phase 3 trial. Lancet Oncol. 2016;17(7):994-1003.

51.	Ansell SM, Lesokhin AM, Borrello I, Halwani A, Scott EC, Gutierrez M, et al. PD-1 blockade with nivolumab in relapsed or refractory Hodgkin's lymphoma. N Engl J Med. 2015;372(4):311-9.

52.	Weintraub K. Drug development: Releasing the brakes. Nature. 2013;504(7480):S6-8.

53.	Kleponis J, Skelton R, Zheng L. Fueling the engine and releasing the break: combinational therapy of cancer vaccines and immune checkpoint inhibitors. Cancer Biol Med. 2015;12(3):201-8.

54.	Postow MA, Callahan MK, Barker CA, Yamada Y, Yuan J, Kitano S, et al. Immunologic correlates of the abscopal effect in a patient with melanoma. N Engl J Med. 2012;366(10):925-31.

55.	Dewan MZ, Galloway AE, Kawashima N, Dewyngaert JK, Babb JS, Formenti SC, et al. Fractionated but not single-dose radiotherapy induces an immune-mediated abscopal effect when combined with anti-CTLA-4 antibody. Clin Cancer Res. 2009;15(17):5379-88.

56.	Kantoff PW, Higano CS, Shore ND, Berger ER, Small EJ, Penson DF, et al. Sipuleucel-T immunotherapy for castration-resistant prostate cancer. N Engl J Med. 2010;363(5):411-22.

57.	Kwon ED, Drake CG, Scher HI, Fizazi K, Bossi A, van den Eertwegh AJ, et al. Ipilimumab versus placebo after radiotherapy in patients with metastatic castration-resistant prostate cancer that had progressed after docetaxel chemotherapy (CA184-043): a multicentre, randomised, double-blind, phase 3 trial. Lancet Oncol. 2014;15(7):700-12.

58. Rooney MS, Shukla SA, Wu CJ, Getz G, Hacohen N. Molecular and genetic properties of tumors associated with local immune cytolytic activity. Cell. 2015;160(1-2):48-61.

59. Alexandrov LB, Nik-Zainal S, Wedge DC, Aparicio SA, Behjati S, Biankin AV, et al. Signatures of mutational processes in human cancer. Nature. 2013;500(7463):415-21.

60. Idorn M, Kollgaard T, Kongsted P, Sengelov L, Thor Straten P. Correlation between frequencies of blood monocytic myeloid-derived suppressor cells, regulatory T cells and negative prognostic markers in patients with castration-resistant metastatic prostate cancer. Cancer Immunol Immunother. 2014;63(11):1177-87.

61. den Brok MH, Sutmuller RP, Nierkens S, Bennink EJ, Frielink C, Toonen LW, et al. Efficient loading of dendritic cells following cryo and radiofrequency ablation in combination with immune modulation induces anti-tumour immunity. Br J Cancer. 2006;95(7):896-905.

62. Waitz R, Solomon SB, Petre EN, Trumble AE, Fasso M, Norton L, et al. Potent induction of tumor immunity by combining tumor cryoablation with anti-CTLA-4 therapy. Cancer Res. 2012;72(2):430-9.

63. Soanes WA, Ablin RJ, Gonder MJ. Remission of metastatic lesions following cryosurgery in prostatic cancer: immunologic considerations. J Urol. 1970;104(1):154-9.

64. Ablin RJ, Soanes WA, Gonder MJ. Elution of in vivo bound antiprostatic epithelial antibodies following multiple cryotherapy of carcinoma of prostate. Urology. 1973;2(3):276-9.

65. Franzese O, Torino F, Fuggetta MP, Aquino A, Roselli M, Bonmassar E, et al. Tumor immunotherapy: drug-induced neoantigens (xenogenization) and immune checkpoint inhibitors. Oncotarget. 2017;8(25):41641-69.

66. Kim K, Skora AD, Li Z, Liu Q, Tam AJ, Blosser RL, et al. Eradication of metastatic mouse cancers resistant to immune checkpoint blockade by suppression of myeloid-derived cells. Proc Natl Acad Sci U S A. 2014;111(32):11774-9.

67. Drake CG, Doody AD, Mihalyo MA, Huang CT, Kelleher E, Ravi S, et al. Androgen ablation mitigates tolerance to a prostate/prostate cancer-restricted antigen. Cancer Cell. 2005;7(3):239-49.

68. Yamoah K, Johnson MH, Choeurng V, Faisal FA, Yousefi K, Haddad Z, et al. Novel Biomarker Signature That May Predict Aggressive Disease in African American Men With Prostate Cancer. J Clin Oncol. 2015;33(25):2789-96.

69. Ross AE, Johnson MH, Yousefi K, Davicioni E, Netto GJ, Marchionni L, et al. Tissue-based Genomics Augments Post-prostatectomy Risk Stratification in a Natural History Cohort of Intermediate- and High-Risk Men. Eur Urol. 2016;69(1):157-65.

70.   Erho N, Crisan A, Vergara IA, Mitra AP, Ghadessi M, Buerki C, et al. Discovery and validation of a prostate cancer genomic classifier that predicts early metastasis following radical prostatectomy. PLoS One. 2013;8(6):e66855.

71.   Piccolo SR, Sun Y, Campbell JD, Lenburg ME, Bild AH, Johnson WE. A single-sample microarray normalization method to facilitate personalized-medicine workflows. Genomics. 2012;100(6):337-44.

72.   Yu J, Yu J, Mani RS, Cao Q, Brenner CJ, Cao X, et al. An integrated network of androgen receptor, polycomb, and TMPRSS2-ERG gene fusions in prostate cancer progression. Cancer Cell. 2010;17(5):443-54.

73.   Robinson JT, Thorvaldsdottir H, Winckler W, Guttman M, Lander ES, Getz G, et al. Integrative genomics viewer. Nat Biotechnol. 2011;29(1):24-6.

74.   Haffner MC, Aryee MJ, Toubaji A, Esopi DM, Albadine R, Gurel B, et al. Androgen-induced TOP2B-mediated double-strand breaks and prostate cancer gene rearrangements. Nat Genet. 2010;42(8):668-75.

75.   Therneau TM, Li H. Computing the Cox model for case cohort designs. Lifetime Data Anal. 1999;5(2):99-112.

76.   Tomlins SA, Alshalalfa M, Davicioni E, Erho N, Yousefi K, Zhao S, et al. Characterization of 1577 primary prostate cancers reveals novel biological and clinicopathologic insights into molecular subtypes. Eur Urol. 2015;68(4):555-67.

77.   Dennis G, Jr., Sherman BT, Hosack DA, Yang J, Gao W, Lane HC, et al. DAVID: Database for Annotation, Visualization, and Integrated Discovery. Genome Biol. 2003;4(5):P3.

78.   Belcaid Z, Phallen JA, Zeng J, See AP, Mathios D, Gottschalk C, et al. Focal radiation therapy combined with 4-1BB activation and CTLA-4 blockade yields long-term survival and a protective antigen-specific memory response in a murine glioma model. PLoS One. 2014;9(7):e101764.

79.   Wilkie KP, Hahnfeldt P. Mathematical models of immune-induced cancer dormancy and the emergence of immune evasion. Interface Focus. 2013;3(4):20130010.

80.   Stone H. Approximation of Curves by Line Segments. Mathematics of Computation. 1961;15(73):40-7.

81.   Koebel CM, Vermi W, Swann JB, Zerafa N, Rodig SJ, Old LJ, et al. Adaptive immunity maintains occult cancer in an equilibrium state. Nature. 2007;450(7171):903-7.

82.   Watson PA, Ellwood-Yen K, King JC, Wongvipat J, Lebeau MM, Sawyers CL. Context-dependent hormone-refractory progression revealed through characterization of a novel murine prostate cancer cell line. Cancer Res. 2005;65(24):11565-71.

83.   Sorrentino C, Musiani P, Pompa P, Cipollone G, Di Carlo E. Androgen deprivation boosts prostatic infiltration of cytotoxic and regulatory T lymphocytes and has no effect on disease-free survival in prostate cancer patients. Clin Cancer Res. 2011;17(6):1571-81.

84.   Morse MD, McNeel DG. Prostate cancer patients on androgen deprivation therapy develop persistent changes in adaptive immune responses. Hum Immunol. 2010;71(5):496-504.

85.   Schaue D, Ratikan JA, Iwamoto KS, McBride WH. Maximizing tumor immunity with fractionated radiation. Int J Radiat Oncol Biol Phys. 2012;83(4):1306-10.

86.   Spitzer MH, Carmi Y, Reticker-Flynn NE, Kwek SS, Madhireddy D, Martins MM, et al. Systemic Immunity Is Required for Effective Cancer Immunotherapy. Cell. 2017;168(3):487-502 e15.

87.   Garon EB, Rizvi NA, Hui R, Leighl N, Balmanoukian AS, Eder JP, et al. Pembrolizumab for the treatment of non-small-cell lung cancer. N Engl J Med. 2015;372(21):2018-28.

88.   Larkin J, Chiarion-Sileni V, Gonzalez R, Grob JJ, Cowey CL, Lao CD, et al. Combined Nivolumab and Ipilimumab or Monotherapy in Untreated Melanoma. N Engl J Med. 2015;373(1):23-34.

89.   Powles T, Eder JP, Fine GD, Braiteh FS, Loriot Y, Cruz C, et al. MPDL3280A (anti-PD-L1) treatment leads to clinical activity in metastatic bladder cancer. Nature. 2014;515(7528):558-62.

90.   Chavin G, Sheinin Y, Crispen PL, Boorjian SA, Roth TJ, Rangel L, et al. Expression of immunosuppresive B7-H3 ligand by hormone-treated prostate cancer tumors and metastases. Clin Cancer Res. 2009;15(6):2174-80.

91.   Parker AS, Heckman MG, Sheinin Y, Wu KJ, Hilton TW, Diehl NN, et al. Evaluation of B7-H3 expression as a biomarker of biochemical recurrence after salvage radiation therapy for recurrent prostate cancer. Int J Radiat Oncol Biol Phys. 2011;79(5):1343-9.

92.   Roth TJ, Sheinin Y, Lohse CM, Kuntz SM, Frigola X, Inman BA, et al. B7-H3 ligand expression by prostate cancer: a novel marker of prognosis and potential target for therapy. Cancer Res. 2007;67(16):7893-900.

93.   Zang X, Thompson RH, Al-Ahmadie HA, Serio AM, Reuter VE, Eastham JA, et al. B7-H3 and B7x are highly expressed in human prostate cancer and associated with disease spread and poor outcome. Proc Natl Acad Sci U S A. 2007;104(49):19458-63.

94.   Powderly J, Cote G, Flaherty K, Szmulewitz RZ, Ribas A, Weber J, et al. Interim results of an ongoing Phase I, dose escalation study of MGA271 (Fc-optimized humanized anti-B7-H3 monoclonal antibody) in patients with refractory B7-H3-expressing neoplasms or neoplasms whose vasculature expresses B7-H3. Journal for ImmunoTherapy of Cancer. 2015;3(2):O8.

95.   Luo L, Zhu G, Xu H, Yao S, Zhou G, Zhu Y, et al. B7-H3 Promotes Pathogenesis of Autoimmune Disease and Inflammation by Regulating the Activity of Different T Cell Subsets. PLoS One. 2015;10(6):e0130126.

96.   Sun X, Vale M, Leung E, Kanwar JR, Gupta R, Krissansen GW. Mouse B7-H3 induces antitumor immunity. Gene Ther. 2003;10(20):1728-34.

97.   Luo L, Chapoval AI, Flies DB, Zhu G, Hirano F, Wang S, et al. B7-H3 enhances tumor immunity in vivo by costimulating rapid clonal expansion of antigen-specific CD8+ cytolytic T cells. J Immunol. 2004;173(9):5445-50.

98.   Lupu CM, Eisenbach C, Lupu AD, Kuefner MA, Hoyler B, Stremmel W, et al. Adenoviral B7-H3 therapy induces tumor specific immune responses and reduces secondary metastasis in a murine model of colon cancer. Oncol Rep. 2007;18(3):745-8.

99.   Hashiguchi M, Kobori H, Ritprajak P, Kamimura Y, Kozono H, Azuma M. Triggering receptor expressed on myeloid cell-like transcript 2 (TLT-2) is a counter-receptor for B7-H3 and enhances T cell responses. Proc Natl Acad Sci U S A. 2008;105(30):10495-500.

100.   Wu CP, Jiang JT, Tan M, Zhu YB, Ji M, Xu KF, et al. Relationship between co-stimulatory molecule B7-H3 expression and gastric carcinoma histology and prognosis. World J Gastroenterol. 2006;12(3):457-9.

101.   Loos M, Hedderich DM, Ottenhausen M, Giese NA, Laschinger M, Esposito I, et al. Expression of the costimulatory molecule B7-H3 is associated with prolonged survival in human pancreatic cancer. BMC Cancer. 2009;9:463.

102.   Crispen PL, Sheinin Y, Roth TJ, Lohse CM, Kuntz SM, Frigola X, et al. Tumor cell and tumor vasculature expression of B7-H3 predict survival in clear cell renal cell carcinoma. Clin Cancer Res. 2008;14(16):5150-7.

103.   Chaudhry A, Rudensky AY. Control of inflammation by integration of environmental cues by regulatory T cells. J Clin Invest. 2013;123(3):939-44.

104.   Galon J, Costes A, Sanchez-Cabo F, Kirilovsky A, Mlecnik B, Lagorce-Pages C, et al. Type, density, and location of immune cells within human colorectal tumors predict clinical outcome. Science. 2006;313(5795):1960-4.

105.   Klyushnenkova EN, Riabov VB, Kouiavskaia DV, Wietsma A, Zhan M, Alexander RB. Breaking immune tolerance by targeting CD25+ regulatory T cells is essential for the anti-tumor effect of the CTLA-4 blockade in an HLA-DR transgenic mouse model of prostate cancer. Prostate. 2014;74(14):1423-32.

106.   Li F, Guo Z, Yu H, Zhang X, Si T, Liu C, et al. Anti-tumor immunological response induced by cryoablation and anti-CTLA-4 antibody in an in vivo RM-1 cell prostate cancer murine model. Neoplasma. 2014;61(6):659-71.

107.   Pardoll DM. The blockade of immune checkpoints in cancer immunotherapy. Nat Rev Cancer. 2012;12(4):252-64.

108.	Topalian SL, Drake CG, Pardoll DM. Immune checkpoint blockade: a common denominator approach to cancer therapy. Cancer Cell. 2015;27(4):450-61.

109.	Weber JS, Yang JC, Atkins MB, Disis ML. Toxicities of Immunotherapy for the Practitioner. J Clin Oncol. 2015;33(18):2092-9.

110.	Tang S, Moore ML, Grayson JM, Dubey P. Increased CD8+ T-cell function following castration and immunization is countered by parallel expansion of regulatory T cells. Cancer Res. 2012;72(8):1975-85.

111.	Kalina JL, Neilson DS, Comber AP, Rauw JM, Alexander AS, Vergidis J, et al. Immune Modulation by Androgen Deprivation and Radiation Therapy: Implications for Prostate Cancer Immunotherapy. Cancers (Basel). 2017;9(2).

112.	Pu Y, Xu M, Liang Y, Yang K, Guo Y, Yang X, et al. Androgen receptor antagonists compromise T cell response against prostate cancer leading to early tumor relapse. Sci Transl Med. 2016;8(333):333ra47.

113.	Dovedi SJ, Adlard AL, Lipowska-Bhalla G, McKenna C, Jones S, Cheadle EJ, et al. Acquired resistance to fractionated radiotherapy can be overcome by concurrent PD-L1 blockade. Cancer Res. 2014;74(19):5458-68.

114.	Young KH, Baird JR, Savage T, Cottam B, Friedman D, Bambina S, et al. Optimizing Timing of Immunotherapy Improves Control of Tumors by Hypofractionated Radiation Therapy. PLoS One. 2016;11(6):e0157164.

Životopis

Benjamin Benzon
Antuna Branka Šimića 13,
21000 Split,
email: benzon.benjamin@gmail.com
Mob: 0976222388

Datum rođenja: 28.12.1987.

• OBRAZOVANJE
2013. - danas   Doktorski studij – Biologija novotvorina, Medicinski fakultet
                                            Sveučilišta u Splitu
2012.   doktor medicine, Medicinski fakultet Sveučilišta u Splitu

• ZAPOSLENJE
2016.- danas asistent na Katedri za anatomiju Zavoda za anatomiju, histologiju i
embriologiju Medicinskog fakulteta Sveučilišta u Splitu

• PRETHODNA ZAPOSLENJA
2013. – 2016 Postdoktorant, Brady Urological Institute, Johns Hopkins University, School
of Medicine, Baltimore, MD, SAD
2012. – 2013.   Staž, Klinički bolnički centar Split

• ZNANSTVENI RAD
- Radenka Kuzmanić Šamija, Dragan Primorac, Biserka Rešić, Bernarda Lozić, Vjekoslav Krželj, Maja Tomasović, Eugenio Stoini, Ljubo Šamanović, **Benjamin Benzon**, Marina Pehlić, Vesna Boraska, Tatijana Zemunik. Association of NOS3 tag polymorphisms with hypoxic-ischemic encephalopathy. *Croat Med J. Jun 2011; 52(3): 396–402.*
- Hurley PJ, Sundi D, Shinder B, Simons BW, Hughes RM, Miller RM, **Benzon B**, Faraj SF, Netto GJ, Vergara IA, Erho N, Davicioni E, Karnes RJ, Yan G, Ewing C, Isaacs SD, Berman DM, Rider JR, Jordahl KM, Mucci LA, Huang J, An SS, Park BH, Isaacs WB, Marchionni L, Ross AE, Schaeffer EM. Germline Variants in Asporin Vary by Race, Modulate the Tumor Microenvironment, and Are Differentially Associated with Metastatic Prostate Cancer*. Clin Cancer Res. 2016 Jan 15;22(2):448-58*
- **B Benzon**, SG Zhao, MC Haffner, M Takhar, N Erho, K Yousefi, P Hurley, JL Bishop, J Tosoian, K Ghabili, M Alshalalfa, S Glavaris, BW Simons, P Tran, E Davicioni, RJ Karnes, K Boudadi, ES Antonarakis, EM Schaeffer, CG Drake, F Feng, AE Ross. Correlation of B7-H3 with androgen receptor, immune pathways and poor outcome in prostate cancer: an expression-based analysis. *Prostate cancer and prostatic diseases 2017 Mar;20(1):28-35*
- Kamyar Ghabili, Jeffrey J Tosoian, Edward M Schaeffer, Christian P Pavlovich, Samad EJ Golzari, Ghazal Khajir, Darian Andreas, **Benjamin Benzon**, Milena Vuica-Ross, Ashley E Ross. The History of Prostate Cancer From Antiquity: Review of Paleopathological Studies. *Urology 2016 Nov ;97:8-12*
- Ana Marija Milat, Ivana Mudnić, Ivica Grković, Nikola Ključević, Mia Grga, Iva Jerčić,1 Diana Jurić, Danica Ivanković, **Benjamin Benzon**, Mladen Boban. Effects of White Wine Consumption on Weight in Rats: Do Polyphenols Matter? *Oxidative Medicine and Cellular Longevity, 2017; 2017:8315803*
- Vujevic M, **Benzon B**, Markic J. New prediction model for diagnosis of bacterial infection in febrile infants younger than 90 days. *Turk J Pediatr. 2017*;59(3):261-268.

- **Benzon B**, Glavaris SA, Simons BW, Hughes RM, Ghabili K, Mullane P, Miller R, Nugent K, Shinder B, Tosoian J, Fuchs EJ, Tran PT, Hurley PJ, Vuica-Ross M, Schaeffer EM, Drake CG, Ross AE. Combining immune check-point blockade and cryoablation in an immunocompetent hormone sensitive murine model of prostate cancer. *Prostate Cancer Prostatic Dis.* 2018 Apr;21 (1):126-136

- Režić-Mužinić N, Mastelić A, **Benzon B**, Markotić A, Mudnić I, Grković I, Grga M, Milat AM, Ključević N, Boban M. Expression of adhesion molecules on granulocytes and monocytes following myocardial infarction in rats drinking white wine. *PLoS One.* 2018 May 10;13(5)